

# **Synchrophasor Based Centralized Remote Synchroscope for Power System Restoration**

Tapas Kumar Barik

Thesis submitted to the faculty of the Virginia Polytechnic Institute and State University in partial  
fulfillment of the requirements for the degree of

**Master of Science**  
**in**  
**Electrical Engineering**

Virgilio A. Centeno, Chair

Jamie De La Reelopez

Vassilis Kekatos

Jan 18<sup>th</sup>, 2018

Blacksburg, VA

Keywords: Phasor Data Concentrators, Synchrophasors, Synchroscope, Voltage Sensitivities,

©Copyright 2018, Tapas Kumar Barik

# Synchrophasor Based Centralized Remote Synchroscope for Power System Restoration

Tapas Kumar Barik

## **Abstract**

The process of Synchronization between two buses in a power system plays a vital role, especially during blackstart or bulk power system restoration period. The synchronization process is primarily monitored in the presence of experienced personnel at the substation level, which might not control or even predict the after effects of synchronization as soon as the synchronizing breaker between the two buses respective to the two islands is closed. However, with the advent of phasor measurement units (PMUs) providing time synchronized synchrophasor data, synchroscope functionality can now be implemented at a centralized remote control platform, usually the control room of the specific utility. This thesis presents a technique along with the actual implementation of such a PMU Synchroscope analytic developed as a part of the Department of Energy sponsored open and Extensible Control and Analytics platform for synchrophasor data (openECA project). The challenges faced to realize this functionality at the centralized remote location along with methods to overcome these hurdles have been discussed in the document. Additional features in comparison to the conventional synchroscope device are also added to facilitate a smoother and successful synchronization, reducing error on behalf of the user /operator and thus, facilitating a faster power system restoration.

# Synchrophasor Based Centralized Remote Synchroscope for Power System Restoration

Tapas Kumar Barik

## **General Audience Abstract**

Successful and proper synchronization between different nodes of a power system is one of the most crucial stages of restoring power after a major wide area electricity outage. Improper synchronization may lead to additional system outages and might delay the restoration process. In this regards, it is desired to perform this vital task at the electric utility's central remote control room. This thesis develops an application to perform the successful reconnection between two nodes of a system overcoming the various challenges and incorporating system delays. The application designed is based on real-time measurements and is integrated with an open source framework platform for ease of the user.

# Acknowledgements

This research work is part of a Department of Energy-sponsored project with Grid Protection Alliance as its chief principal investigator and Virginia Tech and Dominion Energy among its primary project partners. I would like to thank all the entities involved in this project for including me as a part of it.

I would like to express my heartfelt gratitude to my advisor and chair Dr. Virgilio Centeno who provided me with the opportunity to be a part of the openECA project. Without his guidance and supervision, this work would not have been possible. His insights on phasor measurement units helped me to grasp the basic nuances of this project and grow as a student. I would like to thank Dr. Jamie De La Ree and Dr. Vassilis Kekatos who provided a perfect learning environment to set a foundation and strengthen my concepts in basic power system fundamentals.

I would also like to express my gratitude to Dr. Kevin D. Jones from Dominion Energy Virginia who guided me through this project and whose endless discussions on this topic helped me to transform my work from conception to reality. His expertise in coding techniques and synchrophasor based analytics led to the successful implementation of this project.

Lastly, I would also like to thank my family and friends for all their personal and professional guidance, which steered the course of this work in a positive direction for the past two years.

# Table of Contents

<b>Chapter 1- Introduction and History</b> -----	1
1.1 Power system restoration planning-----	1
1.2 Importance of synchronization process-----	2
1.3 Synchrophasor technology and PDCs-----	3
1.3.1 Phasor Measurement Units-----	3
1.3.2 Phasor Data Concentrators-----	4
1.4 The openECA project-----	5
1.4.1 Overview-----	5
1.4.2 Project Partners-----	7
1.4.3 Possible benefits of the project-----	7
1.4.3.1 Value to industry-----	7
1.4.3.2 Value to research community-----	8
1.5 Motivation-----	8
<b>Chapter 2- Traditional synchrosopes and load control techniques</b> -----	12
2.1 Traditional synchrosopes and early work-----	12
2.1.1 Traditional technique-----	12
2.1.2 Electromechanical Synchroscope-----	14
2.1.3 Automatic Synchronizers-----	16
2.1.4 Synchronism-Check Relays-----	17
2.2 Wide Area Control systems (WACS) -----	19
2.2.1 Delays associated with WACS-----	20

2.2.2 Downstream Communication Delays-----	21
2.3 Load Control Technique-----	23
<b>Chapter-3: Algorithm Formulation and Test Setup Implementation-----</b>	<b>26</b>
3.1 Algorithm Formulation-----	26
3.1.1 Calculation of system delays-----	26
3.1.2 Advanced Angle calculation-----	27
3.1.3 Algorithm for the Analytic-----	29
3.1.4 Load control technique based upon voltage sensitivity-----	30
3.2 Implementation and code structure-----	35
3.2.1 Requirements for the application-----	36
3.2.2 Using openECA for creation of project-----	36
3.2.3 C# code implementation for the standalone application-----	38
3.2.3.1 Input Screen Window-----	39
3.2.3.2 Synchroscope Form Window-----	42
3.2.4 Test setup using RTDS simulated data using csv adapters-----	45
3.2.5 Test setup using OPAL-RT ePHASORSIM simulator-----	46
3.2.5.1 Custom modified IEEE 39 bus two-island model-----	48
3.2.5.2 Computational Block-----	51
3.2.5.3 Console Block-----	55
3.2.5.4 Simulink Model configuration in RT-LAB-----	57
3.2.6 Connection of the PMU devices to openECA platform-----	58
3.2.7 Configuring the output channels on the openECA platform-----	59

<b>Chapter 4 - Test Scenarios and Results</b> -----	61
4.1 Validation results using RTDS simulated data-----	61
4.2 Testing results using OPAL-RT ePHASORSIM simulator-----	63
<b>Chapter 5- Conclusion and Future Work</b> -----	76
5.1 Conclusion-----	76
5.2 Future Work-----	77
<b>References</b> -----	78
<b>Appendix - Related Links</b> -----	81

# List of Figures

Fig 1.1: Fundamental Block Diagram of a PMU-----	3
Fig 1.2: Synchrophasor data collection network-----	4
Fig 1.3: Information flow diagram of the system with openECA platform-----	6
Fig 1.4: Information flow diagram of the proposed analytic along with system delays-----	9
Fig 2.1: Typical Synchronizing Panel using the lamp technique-----	13
Fig 2.2: Synchronizing panel with the electromechanical synchroscope-----	14
Fig 2.3: Synchronization Window-----	15
Fig 2.4: Advanced Angle variation-----	17
Fig 2.5: Assisted synchronization system with Synch-check relay-----	18
Fig 2.6: DC control circuit for Synchronizing system used along with Synch check relay-----	19
Fig 2.7: Information flow and delays in WACS-----	20
Fig 3.1: Delay incorporated Advanced Angle representation on the synchroscope-----	28
Fig 3.2: Algorithm for the analytic-----	29
Fig 3.3: Typical QV curve-----	34
Fig 3.4: Main screen of the openECA client webpage-----	37
Fig 3.5: JSON script depicting the I/P and O/P data structures-----	38
Fig 3.6: Main entry point of the code-----	38
Fig 3.7: Initial form of the Input screen window-----	39
Fig 3.8: Code structure for creation of openECA framework-----	40
Fig 3.9: Code Structure for creation of the mapping file-----	40
Fig 3.10: Active measurement Table containing the historian IDs and signal reference IDs-----	41
Fig 3.11: JSON script depicting the I/P and O/P data mappings-----	41

Fig 3.12: Initial form of the Synchroscope form window-----	42
Fig 3.13: Code structure for Update_measurements method-----	43
Fig 3.14: Code structure for TimeIntervalupdate method-----	44
Fig 3.15: Creation of measurement channels for simulated PMUs-----	45
Fig 3.16: Using csv adapter to generate simulated PMUs-----	46
Fig 3.17: Information flow diagram of the testbed setup-----	48
Fig 3.18: Inbuilt ePHASORSIM models for project startup-----	48
Fig 3.19: Original IEEE 39 bus system -----	49
Fig 3.20: Custom modified IEEE 39 bus two-islanded model-----	50
Fig 3.21: C37.118 Simulink model main window-----	51
Fig 3.22: Solver Block (ePHASORSIM product) -----	51
Fig 3.23: Solver function Input file settings-----	52
Fig 3.24: Simulation settings inside the Solver block-----	53
Fig 3.25: Computational subsystem Simulink model architecture-----	54
Fig 3.26: Master driver configuration file-----	54
Fig 3.27: Master driver connection file-----	55
Fig 3.28: Model architecture of the console block-----	55
Fig 3.29: Synchronizing breaker control block-----	56
Fig 3.30: Load control block-----	57
Fig 3.31: Configuration of the simulated PMU devices-----	57
Fig 3.32: Configuration of the phasors of the simulated PMU devices-----	58
Fig 3.33: List of added PMU devices on the openECA platform-----	59
Fig 3.34: Configuring output streams for the breaker commands-----	60

Fig 4.1: RTDS simulated data plots prior and post-synchronization-----	62
Fig 4.2: Synchroscope performance using RTDS simulated data-----	63
Fig 4.3: Test bench setup-----	63
Fig 4.4: Trending real-time simulated measurements on openECA-----	64
Fig 4.5: Input screen window-----	65
Fig 4.6: Analytic Main Window-----	66
Fig 4.7: Synchroscope Form Window prior synchronization-----	66
Fig 4.8: Synchroscope Form Window post synchronization-----	67
Fig 4.9: Voltage phase angle profile prior load control (Scenario-1) -----	69
Fig 4.10: Voltage phase angle profile post load control (Scenario-1) -----	71
Fig 4.11: Voltage phase angle profile prior load control (Scenario-2) -----	73
Fig 4.12: Voltage phase angle profile post load control (Scenario-2) -----	74
Fig 4.13: Smoother synchronization with inclusion of load control-----	75

## List of Tables

Table 2.1: Typical Synch- check parameters-----	18
Table 4.1: Loads at various PQ buses of Area-1 prior load control (Scenario-1) -----	69
Table 4.2: Inertia constants of the various generators in Area-1-----	70
Table 4.3: Loads at various PQ buses of Area-1 post load control (Scenario-1) -----	71
Table 4.4: Loads at various PQ buses of Area-1 prior load control (Scenario-2) -----	72
Table 4.5: Loads at various PQ buses of Area-1 post load control (Scenario-2) -----	74

# **Chapter 1- Introduction and History**

## **1.1 Power system restoration planning**

Power system restoration planning after a wide area system blackout is crucial to improve power system resilience. The wide area power outages and blackouts impact hugely both on the society and economy of the country. It has been estimated that the United States alone incurs a loss of \$20–\$70 billion annually [1] due to power outages. In August 2003, 50 million people lost power for up to two days in the northeastern blackout. This event resulted in the deaths of 11 people and a loss of an estimated \$6 billion [2]. In recent past, weather-induced blackouts in the United States like hurricane Harvey and Irma that hit Texas and Florida and hurricane Maria that hit Puerto Rico, have been testimony about the magnanimity of the impact rendered. Puerto Rico’s apagón, or “super blackout,” is the longest and largest major power outage in modern U.S. history. These outage costs also are dependent upon the duration of outage and outage spread or magnitude. There is a growing need for a more resilient grid that can recover rapidly from the impact of extended power system blackouts following such cascading failures due to extreme weather events or malicious attacks [4].

Power system restoration is categorized into multiple stages: system status determination, plant preparation, generation restoration, transmission path energization, load restoration, and system synchronization [5]. A successful restoration plan should be well designed and thoroughly studied beforehand but still is constrained by operational and technical constraints. Some of the primary objectives driving the restoration plan are minimizing restoration time and service interruptions, maximizing generation capacity and load served, etc. [6].

## **1.2 Importance of synchronization process**

Synchronization of small islands to establish a strong system is a crucial task during the implementation of the abovementioned stages sequentially. Normally, an abnormal or improper synchronization between the two islands might result in one or more of the following effects:

1. High acceleration or deceleration in the prime mover, which increases the transient torque and might damage the rotor.
2. High transient current might flow in the windings.
3. High instant voltages might damage the insulation of the equipment.
4. Power system oscillations might occur due to the transient effect.
5. Possible operation of power system protection devices, which introduce system outages and create additional problems.

Therefore, it is needless to state that a poor or improper synchronization among two islands might worsen the situation even more and might lead to further delays in the power system restoration process. Synchrophasors or PMUs (phasor measurement units) at various measuring sites have now been able to help in this regard, as they are synchronized on a common time base. It provides a direct measurement of system states, which has the potential to benefit power system restoration. During the process of system restoration, PMUs can provide information for both steady state and dynamic conditions [7]. Reports have shown that installed PMUs have made numerous significant contributions to data acquisition during system blackout and system restoration [8, 9]. Moreover, the deployment of PMUs has been strongly recommended by authorities after the Northeast US and Italian blackouts in 2003 [10]. This had also led to the formation of the North American Synchrophasor Initiative in the United States. PMUs have always attracted the power system

researchers due to their wide range of potential applications for system restoration and thus needs to be studied in detail before implementing any synchrophasor-based analytics.

## 1.3 Synchrophasor technology and PDCs

### 1.3.1 Phasor Measurement Units

Integration of Intelligent Electronic Devices (IEDs) to the power system facilitates improved visualization, control, and communication of the power system's performance. At the core, is the development of Wide Area Measurement Systems (WAMS) and Wide Area Monitoring Protection and Control Systems (WAMPACS) that extract consistent and time-accurate measurements from the power system to ensure its stable, secure and economical operation [11]. The core components of the WAMS and WAMPACS are Phasor Measurement Units (PMUs) and Phasor Data Concentrators (PDCs). A Phasor Measurement Unit (PMU) has been defined by the IEEE as “a device that produces synchronized phasor, Frequency, and Rate of Change of Frequency (ROCOF) estimates from voltage and/or current signals and a time synchronizing signal.” Figure 1.1 depicts the fundamental block diagram of a phasor measurement unit.

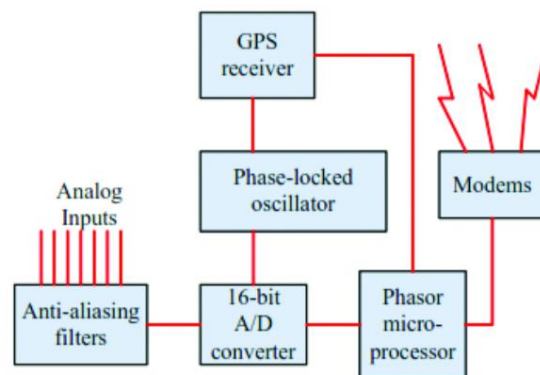


**Fig 1.1:** Fundamental Block Diagram of a PMU

These devices provide a precise and representative view of the power system as they are synchronized to Coordinated Universal Time (UTC) through Global Positioning System (GPS)

signal. Therefore, these devices can provide real-time measurements recorded from different parts of the power system.

### 1.3.2 Phasor Data Concentrators

PDCs are devices able to concentrate measurements from different PMUs, time-align them and communicate them as a single stream to other PDCs or monitoring and control devices. These measurements can be aggregated and time-aligned through PDCs and sent as a single stream of data through the communication network to Supervisory Control and Data Acquisition systems (SCADA) or Energy Management Systems (EMS) [11].

A simple structure of a synchrophasor network consists of phasor measurement units (PMUs) and phasor data concentrators (PDCs) [12] as shown in Figure 1.2.

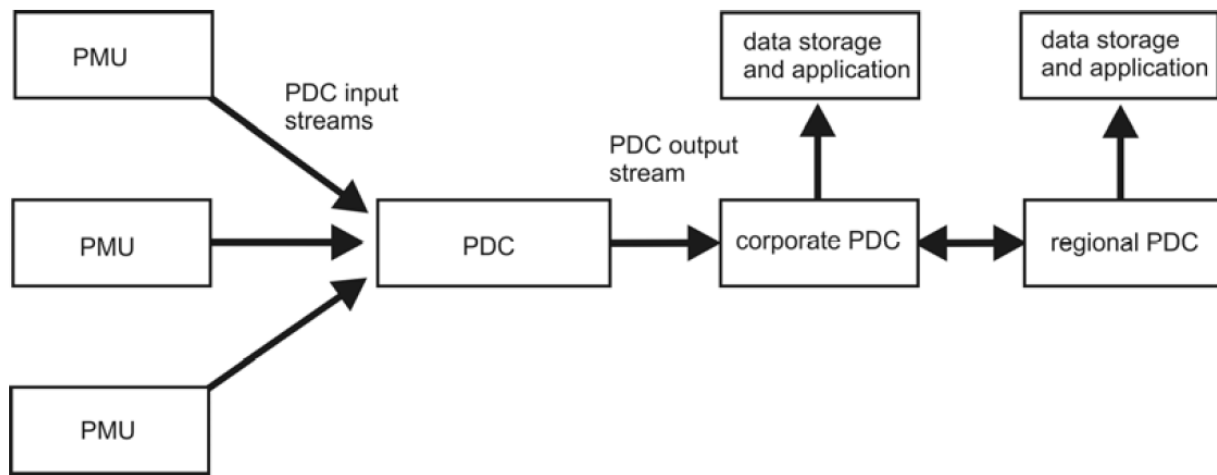


**Fig 1.2:** Synchrophasor data collection network

If multiple PMUs in a substation provide synchrophasor measurements, a local PDC may be placed in the substation. Typically, many PMUs located at various substations receive data and send it in real time to a central PDC at the utility location where the data is collected which may further be sent to other PDCs/synchrophasor systems and/or be used to support many applications, ranging from visualization of information for situational awareness, to applications that provide control or

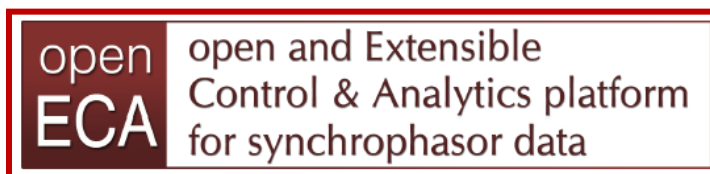
protection functionality. Many PDCs belonging to different utilities can be connected to a common central PDC to aggregate data across the utilities, to provide an interconnection-wide snapshot of the power grid measurements.

A PDC may perform several functions applied to synchrophasor data streams, which might depend on the applications being served by synchrophasor data and the design of the synchrophasor systems. Some of the vital functions of a typical PDC are enumerated as follows:

1. Data aggregation, validation, and forwarding
2. Data transfer protocol support and conversions
3. Data format and coordinate conversion
4. Phase and magnitude adjustment
5. Performance monitoring
6. Redundant and duplicate data handling

## **1.4 The openECA project**

### **1.4.1 Overview**



The objective of the Open and Extensible Control and Analytics (openECA) platform for synchrophasor data project is “to develop an open source software platform that significantly accelerates the production, use, and ongoing development of real-time decision support tools, automated control systems, and off-line planning systems that firstly, incorporates high-fidelity synchrophasor data and secondly, enhances system reliability while enabling the North American Electric Reliability Corporation (NERC) operating functions of reliability coordinator,

transmission operator, and/or balancing authority to be executed more effectively” (Related Links[1] in Appendix).

The openECA platform advances the production deployment of robust and high availability synchrophasor-based software applications by creating a structured approach to the management of real-time and historical synchrophasor measurements within a platform that can effectively handle the most demanding of synchrophasor data system requirements. Figure 1.3 shows the overview of the information flow of the system with the inclusion of openECA.

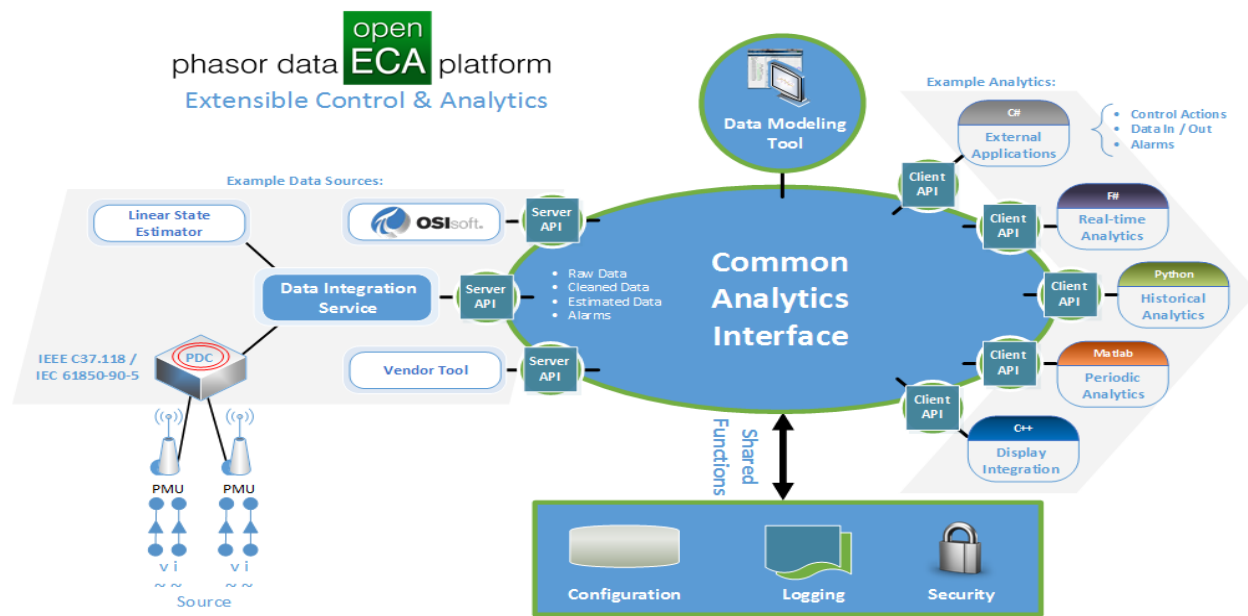


**Fig 1.3:** Information flow diagram of the system with openECA platform

Synchrophasor measurements are aggregated at the Data integration service (PDCs) as shown in the figure and then passed on to the common analytics interface, which basically is the openECA platform. It would act as an interface between measurements and the analytics or different applications built by the power system researchers/developers. The openECA platform provides some starter templates based upon a multitude of languages ranging from MATLAB, Python used commonly in the field of power system studies to C#, C++, F# mostly in the industrial level. This

facilitates the developer not to focus on programming or developing the interface for their applications, rather only focus on their respective analytics and its integration with the platform.

## **1.4.2 Project partners**

This project is a Department of Energy-sponsored project with Grid Protection Alliance as its principal investigator along with the following project partners:

- Dominion Virginia Power
- Virginia Tech
- Oklahoma Gas and Electric
- Southwest Power Pool
- Northwestern Energy
- Bonneville Power Administration
- T&D Consulting Engineers

## **1.4.3 Possible benefits of the project**

### **1.4.3.1 Value to industry**

1. Lowers cost of addition of new production analytic tools.
2. Simplified end-to-end configuration and change management.
3. Improved availability of phasor data with greater visibility of phasor data quality.
4. Robust scalable solution to support phasor data infrastructure of any size.
5. Complements current phasor data architecture and supports integration with other data sources such as SCADA.

### **1.4.3.2 Value to research community**

1. Allows research community to focus on development of new techniques and tools and not on learning how to build information interfaces.
2. Removes barriers to installation of newly developed research tools in production software environments.

## **1.5 Motivation**

As a part of the openECA project, numerous synchrophasor-based analytics were to be developed under the collaboration of Virginia Tech and Dominion Energy Virginia. One of the focus was to use synchrophasor technology for faster power system restoration. As discussed earlier, synchronization of islands is a crucial stage of restoration process especially during blackstart. Normally, the synchronization process is monitored and carried out using a synchroscope at the substation level. A traditional synchroscope is basically a physical piece of hardware used to synchronize two buses or nodes with different frequencies. The restoration procedures generally are planned based on blackstart studies and simulations which are executed earlier and thus follow a predetermined path. Although this path may be pre-determined, one thing that should be considered in the actual implementation is that not all substations are manned and equipped with a synchroscope. This requires the physical transfer of the synchroscope device from one substation to the desired location. This additional activity costs the utility in terms of money and time and significantly limits the flexibility to establish and implement system restoration strategies. Furthermore, the synchronization process is mainly monitored and operated under the surveillance of the experienced substation crews with the help of the synchroscope. Therefore, any technical or human error might lead to unsuccessful or improper synchronization of the two islands. Moreover, as the substations have no control effect on the island's frequency and voltage, carrying out such

a crucial task at the substation level might not provide a bigger picture for controlling or even predicting after synchronization transients /power swings in the system.

However, with the advent of phasor measurement units providing time synchronized synchrophasor data, the synchroscope functionality can now be realized at a centralized remote control platform, usually the control room of the specified utility. Obviously, to achieve such functionality at a remote centralized location, the primary challenge is to overcome the various delays associated with the wide area measurement system. Figure 1.4 depicts the overview of the proposed analytic along with the various delays associated with the system highlighted in red boxes.

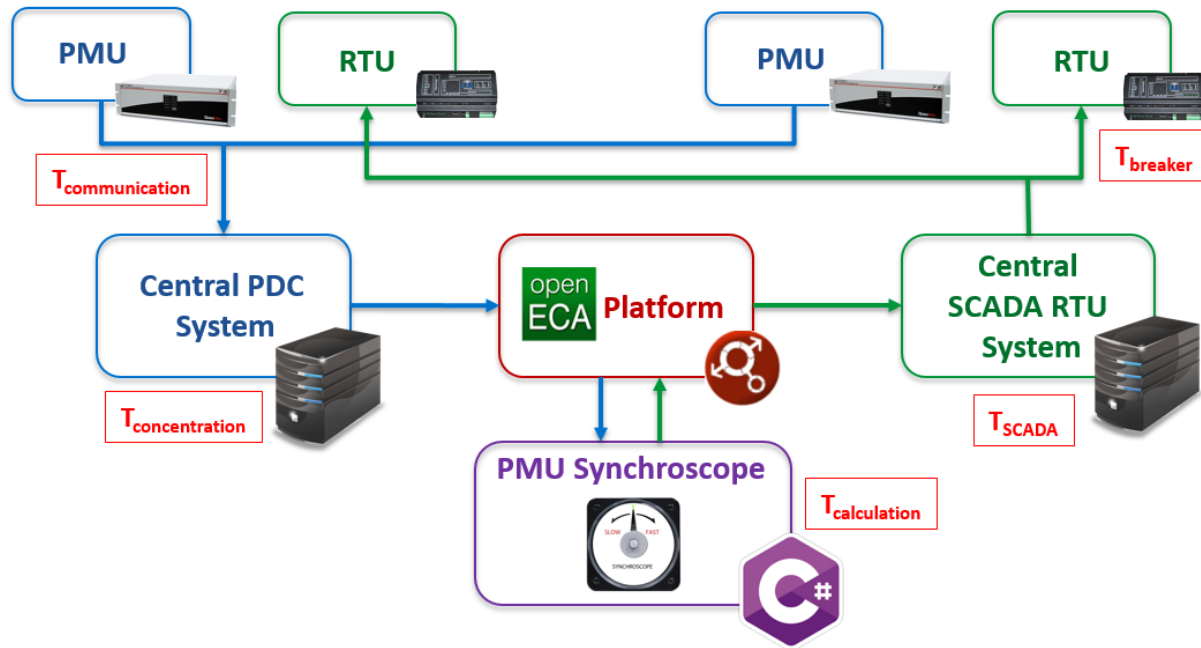


**Fig 1.4:** Information flow diagram of the proposed analytic along with system delays.

Once these delays and their respective variances are determined, a predicted time instant for closing the synchronizing breaker can be calculated to achieve time synchronized breaker closing action at the substation leading to successful synchronization. This thesis presents a technique to implement a modified synchroscope application based upon the openECA platform to be used at

a remote centralized location (hereafter referred to as PMU synchroscope throughout the document for better understanding). The application would predict a particular time instant to initiate the synchronizing breaker close command, overcoming the delays, which might have hindered a proper synchronization activity if not included. Apart from initiating proper breaker command signals, it also raises alarms and annunciations for the convenience of the operators/users to bring the measurements between the two buses within acceptable tolerance limits. The tolerance limits can also be defined by the user/utility depending upon the system parameters and operating conditions.

The methods adopted by the user to achieve these desired results are completely subjected to the discretion of the user/utility. However, as the main focus of this particular work is on bulk power system restoration during which the utility has control over load changes to a flexible extent, this thesis has also presented a technique for an integrated load control technique based upon voltage sensitivities of the load buses in one of the islands in order to bring it closer to the frequency of the reference island or grid. This simply acts as a demonstration of how various techniques can be embedded with this application if required in the future.

The rest of the thesis is organized in the following way:

## **Chapter 2: Traditional synchroscopes and load control techniques**

This chapter presents a literature review of the past work done on synchroscopes, explaining its fundamental functionality. It also discusses the various delay assessment and modeling carried out in the past, which would help us later in the implementation stage of the application. Lastly, it discusses the load control technique finally adopted to be implemented in the analytic.

### **Chapter 3: Algorithm Formulation and Test Setup Implementation.**

This chapter presents with the algorithm developed based on the literature review and findings in chapter-2. Based upon this algorithm, the implementation of the application's code structure is discussed elaborately. Once the standalone application is developed, the chapter then discusses the various test setup configurations required to validate and demonstrate the analytic developed along with its compatibility with the openECA platform.

### **Chapter 4: Test Scenarios and Results.**

This chapter provides the results of the testing of the PMU Synchroscope based upon the various test setups developed in chapter-3. Additionally, the performance of the load control technique adopted is also depicted with observations for the same.

### **Chapter5: Conclusion and Future work.**

The chapter concludes the thesis and summarizes the work completed along with remarks. It also discusses the future work related to this application and recommends several other ideas for expansion of the topic.

# **Chapter-2: Traditional synchrosopes and load control techniques**

## **2.1 Traditional synchrosopes and early work**

Synchronization is the process of matching a source (might be a generator or a small islanded area) with a large existing power system, making it possible to operate these systems in parallel. When two segments of a grid are disconnected, these segments cannot exchange power and share load again until the systems are synchronized and paralleled back together. The synchronization process is usually achieved by an operator, who can synchronize manually or use one of the latest, state-of-the-art automatic synchrosopes (ANSI/IEEE device 25A) [1] and sync-check relays (ANSI/IEEE device 25) to automate closing [13]. The following power system quantities of the incoming source must match the same quantities of the existing or the reference system:

- Phase sequence
- Voltage amplitude
- Frequency
- Phase angle

### **2.1.1 Traditional technique**

One of the oldest techniques of determining if the incoming voltage is in phase with the running voltage is using two lamps connected in series across the phase wires of the incoming and running or reference voltage signals [14] as shown in figure 2.1. The figure below shows a typical synchronizing panel for a generator with two synchronizing breakers. SS1 is the synchronizing

switch that enables synchronizing across Breaker 1. SS2 is the synchronizing switch that enables synchronizing across Breaker 2.

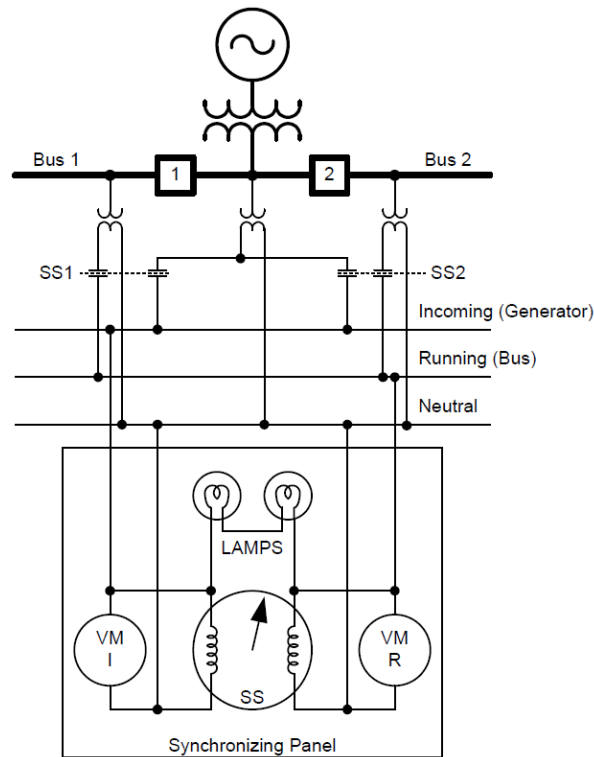


**Fig 2.1:** Typical Synchronizing Panel using the lamp technique

When the two voltages are the same magnitude and angle, the voltage across the lamps will be zero, and they would dim completely out. When the two voltages are 180 degrees out of phase, the lamps will have the two voltages across them added up and burn the brightest. The operator will initiate breaker close when the two lamps are at their dimmest. The slip is indicated by the speed of the lamps cycling between bright and dim phase. If the lamps do not go out completely, it is a fair indicator that the voltage magnitudes are not matched properly. This system provides a fairly crude composite indication of all three parameters that the operator needs to check prior the synchronization process [14].

## 2.1.2 Electromechanical Synchroscope

However to improve visualization of the actual angle between the incoming and running voltages and to improve the response of the operator to synchronize properly, a synchroscope is used in modern synchronizing panels. Figure 2.2 shows an example of an electromechanical synchroscope. The traditional synchroscope does not indicate voltage magnitude difference, so voltmeters for incoming voltage and running voltage are often included. Additionally, frequency meters are sometimes included on the synchronizing panel.

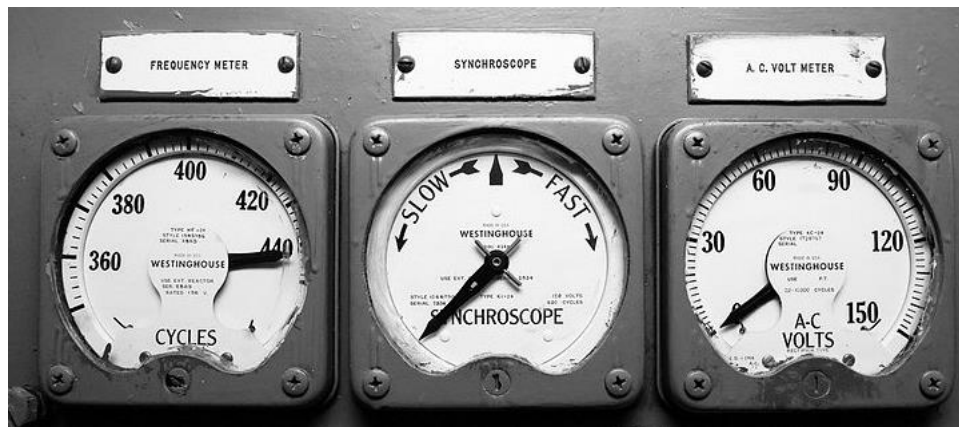


**Fig 2.2:** Synchronizing panel with the electromechanical synchroscope

As seen in the figure, the synchroscope indicates the phase angle difference so that when the two voltages are in phase, the pointer points straight up (12 o'clock position) representing zero degrees. In other words, the 12 o'clock position is the reference bus phasor position and the rotating pointer represents the incoming bus phase angle ( $V_{in}$ ) w.r.t to the reference bus. Therefore, the operator initiates closing the breaker when the phase angle difference between the incoming voltage and the system voltage is close to 0 degrees. When the incoming phasor is running faster than the reference phasor, the pointer rotates in the clockwise direction and vice versa. The revolutions per minute (rpm) of the synchroscope indicates the slip. For example, a synchroscope rotating at 3 rpm equates to 0.05 Hz slip. The operator can determine whether to raise or lower the incoming bus

voltage or frequency based on these indications. The acceptable tolerance limits constitute the synchronization window [13] on the synchroscope device. Figure 2.3 depicts the synchronization window which displays the bus voltage  $V_{ref}$  (running or reference bus), on the vertical axis. Acceptable difference in voltage amplitude limit ( $\Delta V$ ), acceptable phase angle (slip-angle  $\theta$ ) window, in degrees and the acceptable slip frequency,  $\Delta f$ , in hertz are specified differently for different scenarios.

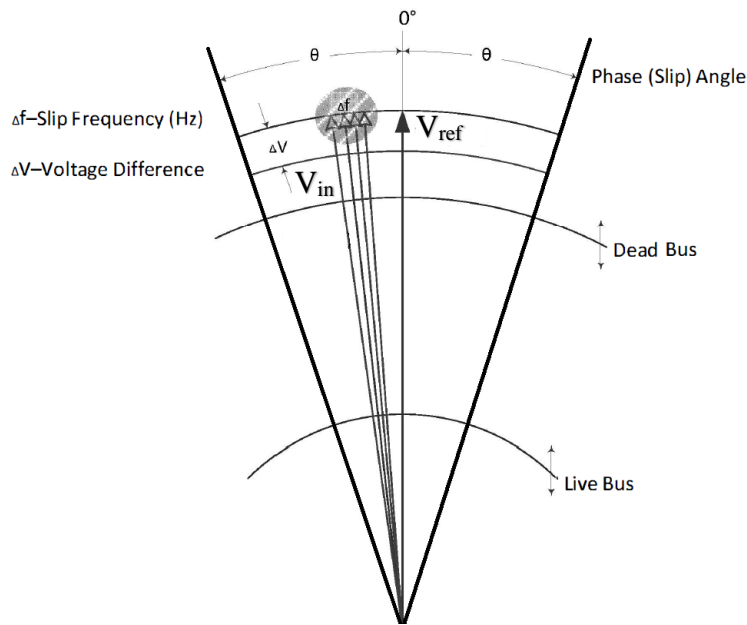


**Fig 2.3:** Synchronization Window

For synchronizing generators with the grid, IEEE Standards C50.12 and C50.13 provide specifications for the construction of cylindrical-rotor and salient-pole synchronous generators, respectively. The limits for both types of generators are specified as:

- Angle  $\pm 10$  degrees.
- Voltage 0 to +5 percent.
- Slip  $\pm 0.067$  Hz.

Narrower tolerance limits produce less system disturbance or power swings and machine damage post synchronization (otherwise known as "softer" synchronization). On the other hand, much

wider tolerance limits allow synchronization to be achieved faster but produce more system disturbance and transients (otherwise known as "harder" synchronization) [13].

The various factors to be considered in deciding these are

- Acceptable power restoration time.
- System loading and operating conditions which depicts its criticality
- Economic aspects regarding damages to the various equipment in the region.

A proper synchronization activity needs to consider these as well as others that are unique to the system. Although it might vary for various systems and the limits might be wider for a two-island synchronization, the point put forth is that the operator would bring the respective quantities as close to each other within the specified limits to ensure a smoother synchronization.

### **2.1.3 Automatic Synchronizers**

Apart from the manual synchronizers, automatic synchronizers (ANSI/IEEE device 25A) are also used primarily for generator synchronization which automatically tries to send the control signals for the governor and automatic speed regulator (AVR) to control (both raise and lower) the output voltage and speed of the generator and to bring it within acceptable limits (within the synchronization window). Traditionally, in the case of manual synchronizer, a good operator judges how fast the phase angle difference is catching up and hence, energizes the breaker close coil accordingly in advance to account for the closing mechanism delay of the synchronizing breaker in such a fashion that the main contacts make as close to a zero-degree angle difference as possible at the time of actual closing in the field . However, the modern automatic synchrosopes measure the slip and calculates what is termed as an advanced angle, which in simple terms is the actual instant to energize the close coil to compensate for the breaker close mechanism delay [14].

The slip-compensated advanced angle is calculated using the following equation:

$$Adv. Ang^{\circ} = 360^{\circ} * Slip * TCLS \quad (1)$$

Where,

*Adv. Ang* is the advanced closing angle (in degrees).

*Slip* is the difference in frequency (in Hz)

*TCLS* is the CB close mechanism delay (in seconds).

Figure 2.4 shows the variation of advanced angle with respect to slip as well as variable breaker closing times.

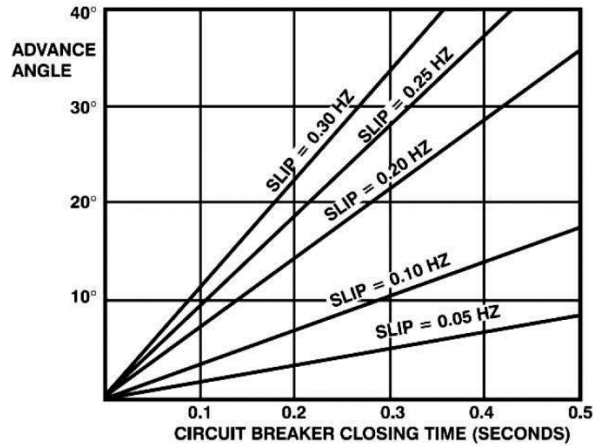


**Fig 2.4:** Advanced Angle variation

Initiation of breaker close commands at this Adv.Ang position would result in a successful synchronization at zero degree phase angle difference between the two buses at the substation. This concept would be primarily used in this document for the development of the synchrophasor based centralized remote synchroscope application.

### 2.1.4 Synchronism-Check Relays

Adding a supervisory relay, known as a synchronism-check (25) relay, to the manual or automatic synchronization process assists with proper and a smoother synchronization. Most synchronism-check relays check that the angle is inside a  $\pm$  angle window and stays there for a time period [14].

The relay cannot control or bring the parameters within acceptable limits and has to be controlled manually or with the help of automatic control. The supervisory relay simply enforces a synchronization window for safe conditions that must be in place before the synchronizing breaker can be closed [13] as shown in figure 2.5.

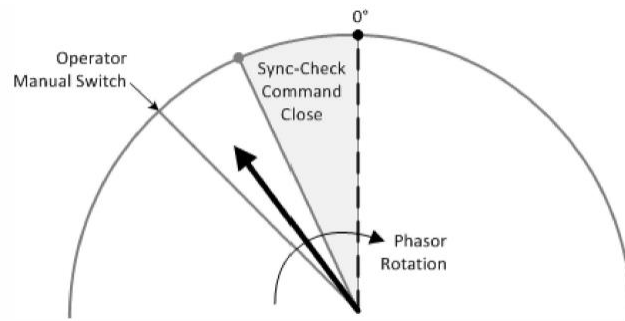


**Fig 2.5:** Assisted synchronization system with Synch-check relay

The synch-check relay compares the voltage difference, slip frequency, and phase angle (slip) differences between the incoming bus and the reference bus. Typical setting ranges for these parameters are depicted in the table below.

Parameters	Typical Value
Voltage difference	$\pm 4\text{V-}8\text{V}$ secondary
Phase (slip) angle	$-25^\circ$ to $+25^\circ$
Frequency slip	$\pm 0.1$ Hz

**Table 2.1:** Typical Synch- check parameters

The supervisory relay does not allow a circuit breaker closure until all of these parameters are satisfied and thus prevents the synchronizing breaker to close out of phase. The synch-check relay output contacts are in series with the operator control switch. Circuit breaker closing occurs only when either the operator manually closes the switch or automatically if an automatic synchronizer is used, and the supervisory relay contacts are closed. The DC control circuit is shown in figure 2.6.

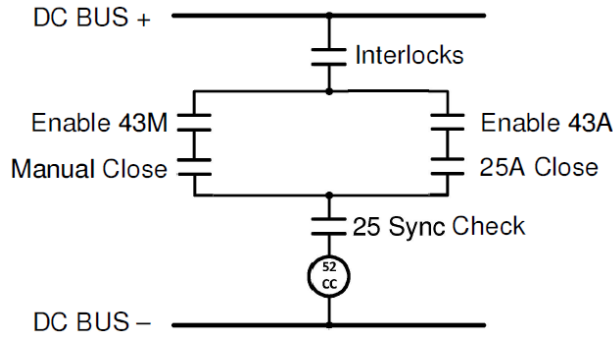


**Fig 2.6:** DC control circuit for Synchronizing system used along with Synch check relay

All these considerations have to be taken into factor while designing a remote synchroscope using synchrophasors. [14] discusses a synchrophasor based synchroscope (PDC synchroscope) in which a dedicated computer running synchrophasor data concentrator (PDC) software can receive streaming data from the various microprocessor-based relays applied for protection and control of the synchronizing breakers. However, it talks about low latency constraint for such a soft synchroscope developed. It also does not incorporate the inclusion of different latency issues in the wide area measurement systems in such an application. To develop a fully functioning generic synchrophasor based centralized remote synchroscope, the different network delays in the system must be considered which are discussed in the following section.

## 2.2 Wide Area Control systems (WACS)

Wide area control systems use the wide area PMU data to control the various electrical and electronic components in the power systems. The application which is developed in this thesis comes within the category of Wide area Control systems. As discussed earlier, the performance of such applications rely upon the communication delays as well as the operational delays present in the WACS and hence, must be predetermined beforehand. Figure 2.7 depicts the information flow and various delays associated with the WACS.

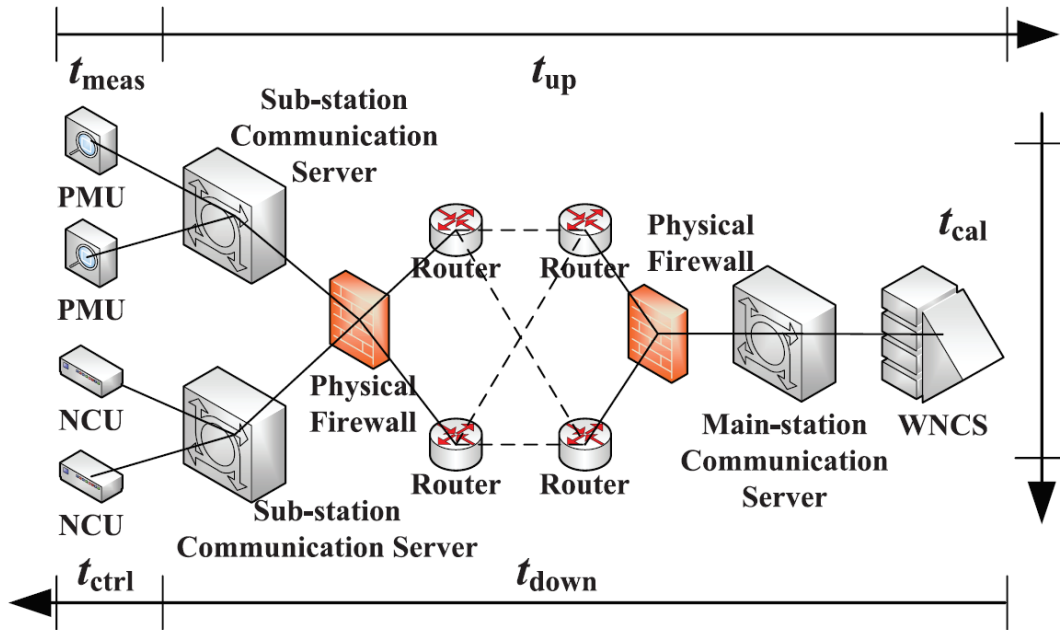


**Fig 2.7:** Information flow and delays in WACS

As shown in the figure, the main components are PMUs, wide area networked control services (WNCS) and networked control units (NCU), acting as sensors, controllers, and actuators respectively.

### 2.2.1 Delays associated with WACS

All the delays associated with the system are categorized into five parts [17]:

1. Measurement delay ( $t_{meas}$ ): It encompasses the signal transferring delay of CTs and PTs, synchronized sampling delay, phasor calculation delay and data packaging and sending delay. Apart from these, the response time of the digital filters in the PMUs increases measurement delays. However, the value is in the order of 10-15 milliseconds and can be termed as constant for our application due to minor variances[17].
2. Data uplink delay ( $t_{up}$ ): It represents the delay to transmit data packets from PMUs to the WNCS through the communication network and the various communication devices such as communication servers and firewalls at various substations.

3. Synchronization and calculation delay ( $t_{cal}$ ): It represents the time required to perform the tasks in WNCS such as receiving and resolving the PMU data packets, synchronizing the data from different PMUs, calculating the control signals, and sending the control data. This delay can be calculated based upon the computational efficiency of the user system.
4. Data downlink delay ( $t_{down}$ ): It is the delay to transmit control data from the WNCS to NCUs. This normally is same as the data uplink delay but might differ if data has to pass through SCADA protocol instead of the faster C37.118 protocol.
5. Controller action delay ( $t_{ctrl}$ ): It includes the delay required for the NCU to receive and resolve the control data packets, and then send the control orders to the breakers. The breaker closing time is also included in this category for simplicity.

Whereas  $t_{up}$  and  $t_{down}$  delays constitute the communication delays,  $t_{meas}$ ,  $t_{cal}$  and  $t_{ctrl}$  constitute the operational delays. As we have discussed above the operational delays are deterministic and can be termed constant for our application. In regards to the communication delays, the upstream delays  $t_{up}$  can usually be derived in our case based upon the difference in time stamp values of the measurements when compared with the time instant it is received by the application. Therefore, the user system at the control center needs to be GPS synchronized with a high precision clock. However, the downstream delay  $t_{down}$  might differ from the  $t_{up}$  if different protocols are used for sending the breaker command signals. Hereafter, our discussion would be mainly focused on the modeling of this downstream delay.

### **2.2.2 Downstream Communication Delays**

The results in [16] calculate the communication latency via different media in the WAMS of the US Pacific Northwest power system: the latency of the fiber optic digital communication was around 38 ms, while the latency using modems over analog microwave channels was over 80 ms.

The communication delay in general varies from a few milliseconds to even hundreds of milliseconds and depends upon various factors, which is discussed in the following sections. The author in [17] proposes an affine model for the communication delays. The communication delay consists of the following delays:

1. Propagation delay ( $\alpha$ ): It is the time required to transmit a packet from the sending port to the receiving port through a particular medium. The delay  $\alpha$  is determined by the transmission media and distance, but not the bandwidth. During the case of synchronization at a particular substation, both these terms are invariant, and thus propagation delay in our case can be termed as a constant.
2. The serial delay ( $\beta$ ): It is the time required to synchronize the bits of a data packet at a certain transmission speed. The delay is proportional to the data packet size ( $L$ ) and inversely proportional to the bandwidth of the link ( $R$ ) [18].

$$\beta = \frac{L}{R} \quad (2)$$

3. The routing delay ( $\gamma$ ): It is the total time that a packet spends at a node, including both the waiting and service time, and is related to the network traffic [17]. As during synchronization procedure, light network traffic would be warranted for smooth functionality, the delay  $\gamma$  can be ignored.

4. The terminal delay ( $\lambda$ ): It includes the delays caused due to physical firewalls and communication servers on each side of the channel. These delays can also be treated as a constant.

So for  $j$  nodes and  $k$  links in a channel for the downstream communication, then  $t_{down}$  can be written as:

$$t_{down} = \sum_{i=1}^k \alpha_i + \sum_{i=1}^j \beta_i + \sum_{i=1}^j \gamma_i + 2\lambda \quad (3)$$

As discussed above, the propagation and terminal delays can be clubbed together as a constant and routing delay can be neglected, the final equation defining the affine evaluation model(AEM) for communication delays, varying linearly as the size of the data packets for light network conditions is represented as:

$$t_{down} = T_o + \frac{L}{R} \quad (4)$$

Where,

$$T_o = \sum_{i=1}^k \alpha_i + 2\lambda \quad (5)$$

The above defined AEM would be used to model the downstream communication delays. Firstly, as discussed in [17], several groups of measurement data for  $t_{down}$  are taken with different L in a channel. Second, the average of each group of  $t_{down}$  is calculated. Finally, the parameters  $T_o$  and R of AEM are calculated by linear fitting. The measurement method of these  $t_{down}$  is separately explained in the next chapter.

## 2.3 Load Control Technique

The literature review for the implementation of the PMU synchroscope has been discussed in the earlier sections. However, the synchroscope to be designed does not have the capability to automatically change the voltage and frequency of the island under observation. Conventional synchrosopes send control signals for the governor and AVR of the generator to bring the parameters within the limit. As the PMU synchroscope application deals with island synchronization in general (which also can be used for generator synchronization), control schemes have been out of the context for this project as each scenario would be different and has to be tailor-made for control of frequency and voltage of the power source (single generator or an island) to be synchronized. Therefore, to demonstrate a generic functionality of control measures,

an add-on functionality is included in this thesis work, as a representation of the control measures, which might be used by the operator in the utility. Although the utility might have other control measures to achieve the same, the following work intends to show how a generic system-wide control measure can be used in conjunction to the PMU synchroscope to achieve smoother synchronization with minimal power swings after synchronization. Moreover, as voltage control methods are being developed as a part of several separate analytics in the openECA project, the main focus would be frequency control of the island which must consider both frequency and voltage measurements for better analysis. One of the important assumptions made in this context is that even if the PMU synchroscope developed can be used for either black start or normal synchronization procedure, the main focus of the analytic or motivation was for bulk power system restoration. Therefore, it would be safe to assume that during this situation, the utility has huge control on the load and can be modified to a larger extent at the time of blackstart operation or load rich islanded system. This might not be true for a normal synchronization procedure, and the utility might use generation control to achieve this. However as stated earlier, generator governor control is tailor made for separate generators and therefore, the add-on functionality depicted in this document focusses on how a generic control method such as a load control technique can be integrated with the PMU synchroscope.

Based on the above assumption, a technique stated in [21] is discussed and implemented in the document. Although the technique stated in [21] deals with load shedding, the main reason to adopt this technique is that it focusses on a load shedding scheme which not only corrects the system frequency but also improves the voltage profile throughout any system which can be modified to meet the requirements of the synchroscope application. The main purpose of this method is that it considers the rate of change of frequency and the voltage sensitivities before implementing the

actual load shedding scheme which is beneficial for the situation at hand. The scheme is simple and does not involve complicated calculations. It has proved to be successful in restoring the frequency within its pre-defined limits and henceforth would be discussed in the next chapter in a modified fashion to suit our requirements and not simply on load shedding. A quick summary of the method is stated as follows.

The first step is the measurement stage which collects the voltage values along with the rate of change of frequency values at each bus. When a disturbance causes a deviation in frequency or a change in bus voltage or both, it is recorded, and the magnitude of the disturbance is estimated using the power swing equation. This determines the amount of load to be shed finally. Once, the quantity of load to be shed is decided, the buses are ranked according to their  $dV/dt$  values. This ranking decides the order in which load will be shed. Therefore, the bus where the voltage is declining at a faster rate has a higher  $dV/dt$  value and is ranked at a higher position. Once the order of the shedding is decided the next stage calculates how much load needs to be shed from each load bus. This is decided by a formula based on the voltage sensitivities [21] (otherwise called as V-Q sensitivity) based upon the V-Q curve analysis. System planners conduct numerous studies using the V-Q curve to determine the amount of load that needs to be shed to retain voltage stability. Finally, load shedding may be manual or automatic. However, for the sake of the work stated in this document, this particular load shedding technique has been modified and now applied to both load increase as well as load shedding to bring the frequency of the incoming island close to the running or reference island which is discussed in the algorithm section of chapter-3.

# Chapter-3: Algorithm Formulation and Test Setup

## Implementation

### 3.1 Algorithm Formulation

#### 3.1.1 Calculation of system delays

As discussed in the previous chapter, the various delays in the system are constant and can be calculated easily except the communication delays. However, we can calculate the actual communication delays associated with the system beforehand using an affine evaluation model (AEM) using Eqn. 4. For calculation of those parameters and measurement of the communication delays, the method suggested in [17] can be implemented as follows:

**Step-1:** Data packets conforming to actual PMU data sizes are constructed. Then the sending server, which is at the same port as the WAMS server in the control center, sends the constructed data packets to the receiving server, which is at the same port as the PMU.

**Step-2:** The receiving server returns the data packets immediately after receiving the packets. The sending server times the sending and receiving operations by a local timer.

**Step-3:** The time intervals are calculated which is twice the communication delays. The statistics of the communication delays can be obtained from the various groups of measurement tests.

In an alternative method, timestamped data packets are sent from the control server (in our case the openECA instance at the control center), and another openECA instance at the substation level receives these data packets. Measuring the difference in timestamps of the received data packets with the coordinated universal time, we can measure the average value of the downstream

communication delays, which would be then fed into the application to calculate the advanced angle as discussed earlier. It should be noted that the variances in the communication delays are relatively insignificant to affect the functionality of the synchroscope and hence are neglected, which is discussed in the next section.

### 3.1.2 Advanced Angle calculation

Once the synchronization path is adopted, and the downstream delays in that particular path are estimated, the mean value of the delay can be fed to the core algorithm of the analytic. To include this delay in the system, we use the concept of advanced angle as discussed in the earlier chapter as used for automatic synchronizers, which is the representation of the movement of the voltage phasor of the incoming bus with reference to the voltage phasor of the reference bus in regards to the delays associated. In other words, it provides a predicted angle or position for the rotating phasor hand of the synchroscope if these delays are considered and the all the other parameters of the system are kept constant or stable.

The advanced angle is now modified and is a function of the cumulative delays (which includes all the upstream as well downstream delays in addition to the breaker closing time) and the associated slip in frequency between the two buses to be synchronized. It is represented by the equation as shown below:

$$Adv. Ang^{\circ} = 360^{\circ} * Slip * Cumulative Delays \quad (6)$$

$$Cumulative Delays = operational delays + t_{up} + t_{down} + TCLS \quad (7)$$

Where,

*Adv. Ang* is the advanced closing angle (in degrees).

*TCLS* is the CB close mechanism delay (in seconds).

$t_{up}$  is the upstream delay (in seconds).

$t_{down}$  is the downstream delay (in seconds).

Diagrammatically, the advanced angle can be depicted in the following figure.

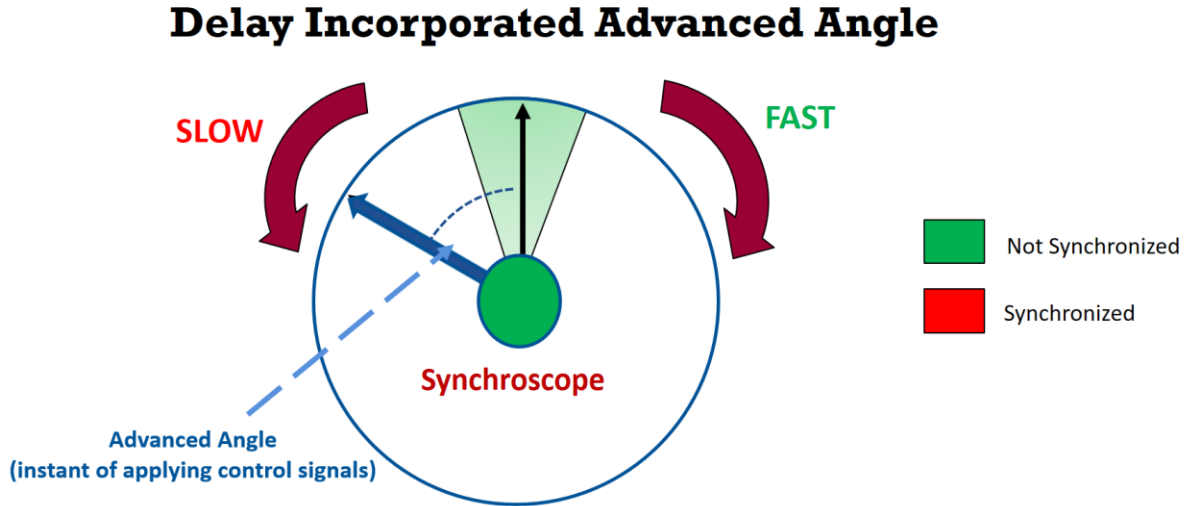


**Fig 3.1:** Delay incorporated Advanced Angle representation on the synchroscope

The position of the advanced angle might move clockwise or anticlockwise depending whether the incoming phasor frequency is lesser or greater than the reference phasor frequency respectively. Once this advanced angle is calculated, the phase angle tolerance limits are added and subtracted from this angular position, and the modified angle tolerance window or a modified synchronization window is formed across this position. In this fashion, the actual predicted modified angle tolerance window would be formulated, in which breaker close commands can be initiated in such a manner that the actual closing breaker instant at the substation will be with minimal phase angle difference, i.e. within the original phase angle tolerance window (as depicted by the green pie region in figure 3.1). It should be noted that for initiation of the synchronizing breaker close command, other conditions should also be met as discussed earlier.

### 3.1.3 Algorithm for the Analytic

The algorithm for the application is depicted in the form of a flowchart in the following figure.

## Algorithm

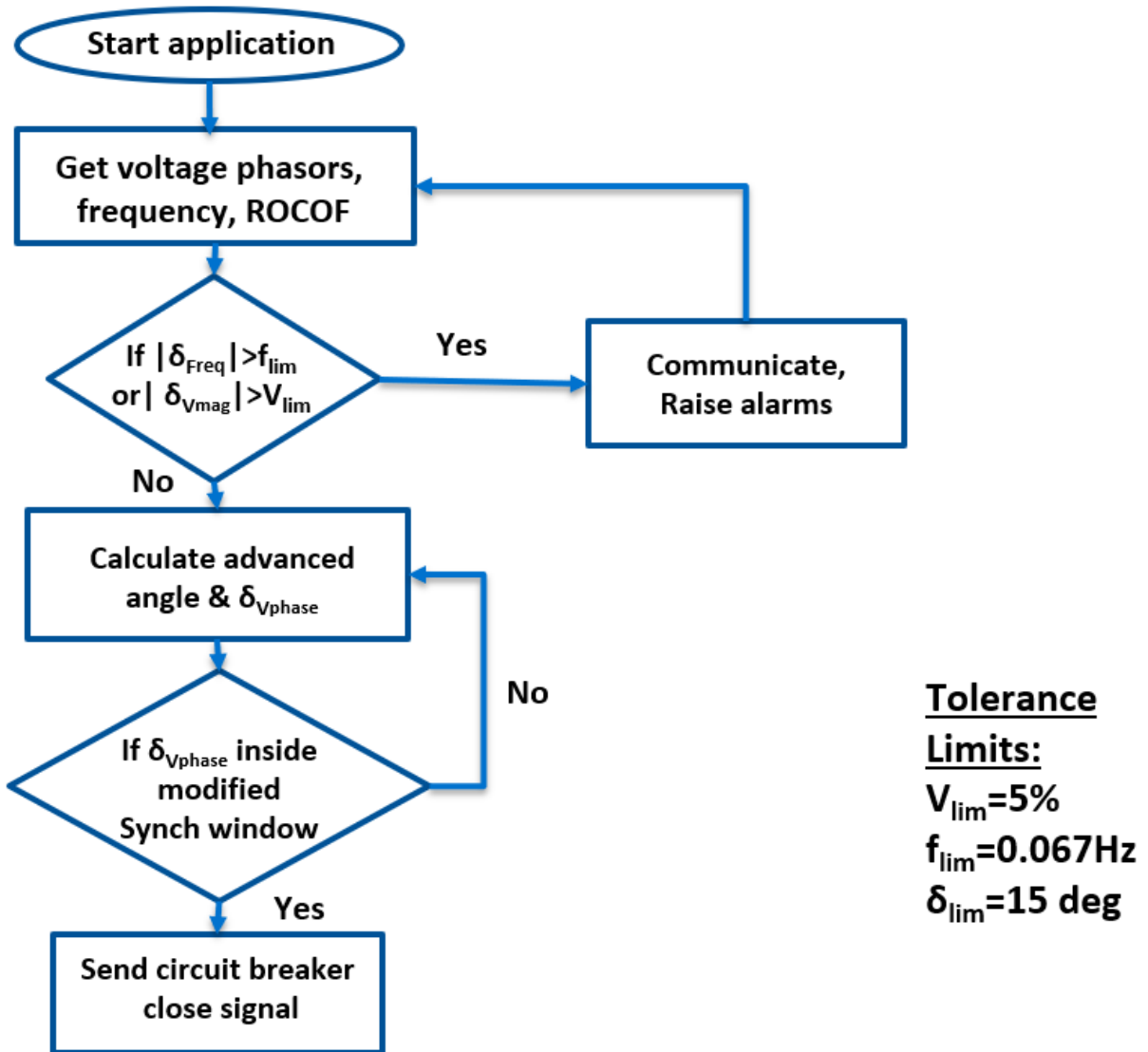


Fig 3.2: Algorithm for the analytic

The algorithm can be stated as follows:

1. The synchrophasor measurements of the two buses to be synchronized, which include the voltage phasor measurements as well as frequency and rate of change of frequency (ROCOF) are streamed into the application.
2. If the difference in voltage magnitude and frequency measurements between the two buses is beyond the user-specified limits, proper alarms and annunciations are raised and communicated to the user.
3. Once the user takes the necessary actions and brings the measurements within acceptable tolerance limits of each other, the voltage phase angle difference is checked continuously to lie inside the modified synchronization window calculated based upon the advanced angle calculated and the phase angle tolerance limits.
4. At this stage, breaker close command is initiated either manually by the user or automatically generated by the analytic at the advanced angle angular position to finally close the breaker at zero degrees phase angle difference after the cumulative delays have elapsed.

### **3.1.4 Load control technique based upon voltage sensitivity**

As discussed in the earlier chapter, the load control technique which is being integrated into this project as a part of a demonstration of how frequency control measures can be incorporated along with the analytic, is being derived from the load shedding technique provided in [21].

The whole algorithm is divided into three steps:

#### **Step-1: Calculation of total load change**

The main motive is to bring the incoming phasor frequency ( $f_{\text{incoming}}$ ) close to the reference phasor frequency, and thus all the control measures are restricted to the incoming island and its generators and loads. The first step is to estimate the total amount of load to be modified for achieving this

desired frequency ( $f_{reference}$ ). This can be calculated using the swing equation. Normally, the swing equation for a particular generator can be written as follows:

$$\frac{2H}{\omega_s} \frac{d^2 \delta}{dt^2} = P_m - P_e \quad (8)$$

It can be modified and written as,

$$\Rightarrow \frac{2H}{f_0} \frac{df}{dt} = P_m - P_e = P_{diff} \quad (9)$$

where,

$H$  is the inertia constant of the generator.

$\delta$  is the internal angle of the generator otherwise known as load/power angle.

$\omega_s$  is the synchronous angular velocity of the generator.

$f_0$  is the nominal frequency of the system.

$P_m$  is the mechanical input power to the generator.

$P_e$  is the electrical output power of the generator.

This equation is valid for a single generator. For a multi-machine system in an island which swings together, the swing equations can be combined. Such machines are called as coherent generators. The equivalent inertia constants, mechanical input and electrical output power to the overall system (consisting of  $n$  generators) can be written as:

$$H_{eq} = \sum_{i=1}^n H_i \quad (10)$$

$$Pm_{eq} = \sum_{i=1}^n Pm_i \quad (11)$$

$$Pe_{eq} = \sum_{i=1}^n Pe_i \quad (12)$$

Where,

$H_{eq}$  is the equivalent inertia constant of the whole island containing  $n$  generators.

$Pm_{eq}$  is the equivalent mechanical input power for the multi-machine islanded system.

$Pe_{eq}$  is the equivalent electrical output power or load for the multi-machine islanded system.

So,

$$Pdiff_{eq} = Pm_{eq} - Pe_{eq} \quad (13)$$

$Pdiff_{eq}$  is the total modification in the load consumption required to achieve the desired frequency within a stipulated time period  $t_{diff}$  as decided by the utility based upon the convenience and availability of loads.

Therefore, a derivation from the modified swing equation for the multi-machine system can be written as:

$$\frac{2H_{eq}}{f_0} \frac{\Delta f}{\Delta t} = Pdiff_{eq} \quad (14)$$

Where,

$$\frac{\Delta f}{\Delta t} = \left( \frac{f_{incoming} - f_{reference}}{t_{diff}} \right) \quad (15)$$

The time  $t_{diff}$  and thus the necessary average rate of change of frequency needed to achieve the desired frequency after the predefined overall load change can be decided by the utility depending upon restoration capability. For achieving a larger change in frequency within a stipulated time, the rate of change of frequency and hence the load change should be higher and vice versa. In this way, the total load change required in the islanded system can be calculated.

### **Step-2: Ranking the load buses for modifying load.**

Now once, we have the total load change desired, the various load buses are ranked in order of priority to have their share of load changed. This was carried out on the basis of  $dV/dt$  values in

the original paper in case of a disturbance. However, for the sake of this project, the priority would be based on sheer voltage magnitudes at the load buses. In other words, if the overall load is to be shed at each load bus, the bus with the lowest voltage magnitude is given priority first which makes sense as the voltage profile of the bus with the lowest voltage magnitude should be alleviated sooner. On the other hand, if the overall load is to be increased at each load bus, the bus with the highest voltage magnitude is chosen first for the addition of load followed by others. However, the user in the utility might follow this scheme or might not depending upon convenience and load availability conditions at that particular time.

**Step-3: Allocating the % share of load change for each load bus.**

Now, once the overall load change required for matching the frequencies of the two islands along with a ranking of the load buses is calculated, the next task is to allocate the % share of load change for each load bus within the island. This is done based on the voltage sensitivity factor of each load bus which is calculated based on the QV analysis. Now the QV analysis is carried out in the following manner.

The equations for active and reactive power injections at a particular bus (i) are formulated as:

$$P_i = \sum_{j=1}^n |V_i||V_j||Y_{ij}|\cos(\delta_{ij} - \theta_{ij}) \quad (16)$$

$$Q_i = \sum_{j=1}^n |V_i||V_j||Y_{ij}|\sin(\delta_{ij} - \theta_{ij}) \quad (17)$$

QV analysis provides the relation between the change in voltage at a bus dependent upon the reactive power change at that particular bus. Therefore taking the derivative of  $Q_i$  with respect to  $V_i$ , we get

$$\frac{dQ_i}{dV_i} = \sum_{j=1}^n |V_j||Y_{ij}|\sin(\delta_{ij} - \theta_{ij}) \quad (18)$$

This is termed as the voltage sensitivity of V-Q sensitivity of the bus. Now, if we look into a typical QV curve as shown in figure 3.3, the knee point (voltage collapse point) of the plot denotes that the system is in a critical situation and is unstable beyond that point. As the knee point is approached, the  $dQ/dV$  values become smaller and close to zero. Thus, a system bordering on instability will have a small value of the slope at the knee point and having a high positive value of slope and away from the knee point would indicate high stability.

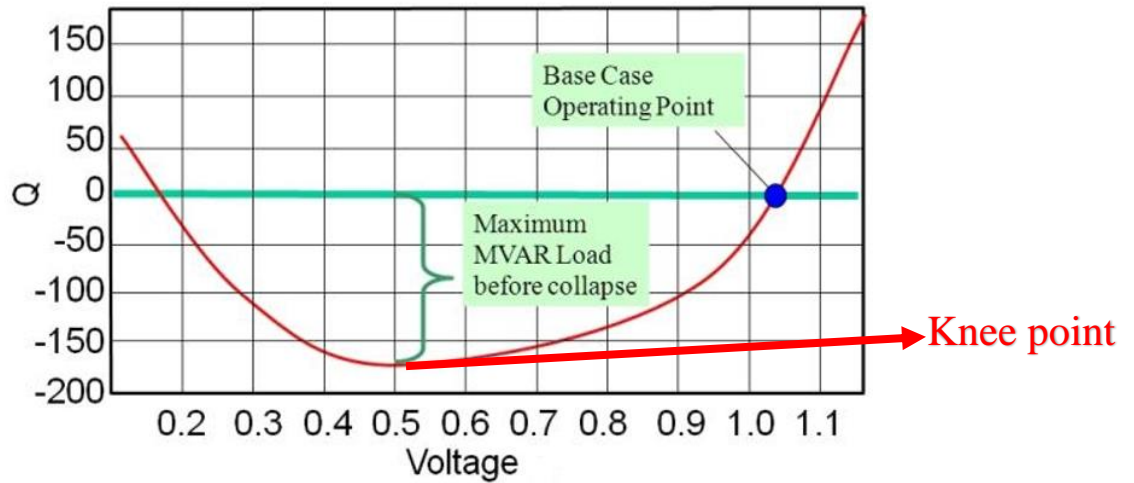


**Fig 3.3:** Typical QV curve

Therefore, a higher amount of load shed is warranted for the buses having lesser voltage sensitivity value and vice versa for load increase case. In other words, for load shed or decrease case:

$$\frac{dQ_i}{dV_i} \text{ is inversely proportional to the load shed}$$

or,

$$\frac{dV_i}{dQ_i} \text{ is directly proportional to the load shed}$$

Now, the load shed at each bus is a fraction of the total load required to be shed to maintain the power balance. This fraction of the load at each bus is proportional to the fraction of the  $dV/dQ$  value at each bus with respect to the sum of all  $dV/dQ$  values calculated for all buses.

Thus, the load change at each load bus in the load decrement scenario is represented as:

$$Loadchange_i = \frac{\frac{dV_i}{dQ_i}}{\sum_{j=1}^n \frac{dV_j}{dQ_j}} * Pdiff_{eq} \quad (19)$$

Similarly, for the load increment case,

$$Loadchange_i = \frac{\frac{dQ_i}{dV_i}}{\sum_{j=1}^n \frac{dQ_j}{dV_j}} * Pdiff_{eq} \quad (20)$$

Where,

n= total number of load (PQ) buses

Finally, we have allocated the % share of load change to be modified at each load bus depending upon the scenario. All the above algorithms are implemented for the creation and functioning of the analytic as discussed in the following section.

## 3.2 Implementation and code structure

This section and the following sections portray the work completed as the part of the application developed based upon the algorithm as discussed in the earlier section in C# and submitted in accordance to the results of the openECA project. The important aspect of an open source application is that any user can access the code and tweak as he or she deems fit. One important thing to keep in mind is that the code should be structured in a way, which can be easily readable and understandable for a power systems engineer who might not have much exposure to C# language. All these considerations are taken into account, and proper comments are provided alongside in the code. The application is designed in such a way that it can be easily implementable and used on the openECA platform and can retrieve PMU data from either simulations or real field data. Also, extensive documentation is created and uploaded along with the project source code on GITHUB for the ease of any user/operator. The application itself is developed in C# but in the

later section, load control technique using voltage sensitivity analysis is carried out in MATLAB SIMULINK, and the process of implementation is presented too.

### **3.2.1 Requirements for the application**

The main application of the standalone PMU synchroscope should be capable of performing the following functions:

1. Establish a connection with openECA platform.
2. Configure the incoming and reference buses for the proper functioning on the fly, so that it can be re-used and can perform multiple synchronizations whenever necessary.
3. Retrieve the necessary PMU data from the selected buses from the openECA instance.
4. Follow the algorithm and raise proper annunciations if values are out of bounds.
5. Initiate proper commands if all conditions are satisfied and publish the data to the openECA output channel.

### **3.2.2 Using openECA for creation of project**

The openECA software was downloaded from the GITHUB site. The links for all the materials and source code are provided in the appendix section. Once the openECA software is installed on the system, two applications are installed simultaneously on the system namely openECA manager and openECA client. The openECA manager acts a visualization tool for the different devices added to the database of openECA. It supports the manual addition of measurement channels and configuring different PMU devices to be added to the openECA database. Once the necessary measurement channels are created in the openECA manager, the openECA client is executed which directs to a webpage as shown in figure 3.4 where the initial project for the application is created.

Counter	Last	Average	Maximum	Units
CPU Utilization	2.69	7.31	27.97	Average % / CPU
I/O Data Rate	0.00	565.38	4898.46	Kilobytes / sec
I/O Activity Rate	0.00	162.42	1187.57	Operations / sec
Process Handle Count	973.00	966.78	1058.00	Total Handles
Process Thread Count	32.00	37.59	45.00	System Threads
CLR Thread Count	15.00	19.53	25.00	Managed Threads
Thread Queue Size	0.00	0.00	0.00	Waiting Threads
Lock Contention Rate	0.00	0.00	0.00	Attempts / sec
Process Memory Usage	103.52	92.41	106.66	Megabytes
CLR Memory Usage	22.55	13.92	22.55	Megabytes
Large Object Heap	12.47	7.47	12.47	Megabytes
Exception Count	85.00	55.88	85.00	Total Exceptions
Exception Rate	3.77	1.52	14.33	Exceptions / sec
IPv4 Outgoing Rate	2.82	3.35	20.81	Datagrams / sec
IPv4 Incoming Rate	0.00	1.99	10.66	Datagrams / sec
IPv6 Outgoing Rate	11.28	57.71	2071.28	Datagrams / sec
IPv6 Incoming Rate	0.00	0.39	9.48	Datagrams / sec

Statistics calculated using last 120 counter values sampled every second.

**Fig 3.4:** Main screen of the openECA client webpage

Under the “Manage Data structures” tab, the respective input and output data structures are defined. The PMU synchroscope application is concerned with voltage phasors and frequency measurements only. Therefore, voltage phasors containing voltage magnitude and phase angles and frequency of the buses concerned are defined as the input data structures.

After defining the data structures, the input and output mappings are managed (as highlighted in figure 3.4). The function of these mappings is that it maps the data of the desired measurement channels to the defined data structures. Once the mappings are done, the next step is to generate a project (under the Generate Project tab in figure 3.4) with these input and output mappings. openECA provides many starter project templates which can use a multitude of software languages. For this particular work, C# language was chosen in order to generate the project. In the openECA workspace on the user system, a C# project is generated which is a project template to build the rest of the application as desired. An example of the input and output data structure,

required for the application can be viewed in the form of a JSON (JavaScript Object Notation) script named “UserDefinedTypes.ecaidl” file in the model file of the project generated.

```

category GPA
test_DataIn {
    FloatingPoint Double test_VoltMag1
    FloatingPoint Double test_VoltAng1
    FloatingPoint Double test_VoltMag2
    FloatingPoint Double test_VoltAng2
    FloatingPoint Double test_Incoming_freq
    FloatingPoint Double test_Reference_freq
    FloatingPoint Double Roc_incoming_phasor
    FloatingPoint Double Roc_Reference_phasor
    FloatingPoint Double test_CB_status
}

category GPA
test_DataOut {
    FloatingPoint Double CB_close
    FloatingPoint Double CB_open
}

```

**Fig 3.5:** JSON script depicting the I/P and O/P data structures

### 3.2.3 C# code implementation for the standalone application

The complete order of the code structure is discussed in this section. The initial entry point to the main code is the “Program.cs” file (Figure 3.6) which calls the “Input screen” window where the user can provide the bus measurements and configure on the fly.

```

namespace PMU_Synchroscope
{
    static class Program
    {
        /// <summary>
        /// The main entry point for the application.
        /// </summary>
        [STAThread]
        static void Main()
        {
            Application.EnableVisualStyles();
            Application.SetCompatibleTextRenderingDefault(false);
            Input_screen inputscreen = new Input_screen();
            Application.Run(inputscreen);
        }
    }
}

```

**Fig 3.6:** Main entry point of the code

### 3.2.3.1 Input Screen Window

The input screen allows the user to provide the following data as depicted in figure 3.7 :

1. Signal reference IDs of the incoming and reference phasor voltage magnitude, phase angle, frequency, the rate of change of frequency measurements.
2. Signal reference IDs of the synchronizing breaker close and open command and its status measurement channel.
3. Tolerance limits for voltage magnitude difference, phase angle difference and slip in frequency as desired by the user/operator.

The screenshot shows a software window titled "Input screen" with a title bar containing standard Windows window controls. The main content area is titled "PMU Synchroscope" and contains the following elements:

- A central instruction: "Enter the Signal Reference for the following data".
- Two columns of dropdown menus under the heading "Enter the Signal Reference for the following data":
  - Incoming Phasor Data:** Frequency, Voltage Magnitude, Voltage Angle, ROCOF.
  - Reference Phasor Data:** Frequency, Voltage Magnitude, Voltage Angle, ROCOF.
- A section titled "Synchronizing Breaker Data" with a dropdown menu for "Synchronizing Breaker Status".
- Two dropdown menus for "Breaker close command" and "Breaker open command".
- An "ENTER" button.
- A section titled "Tolerance Limits" with the instruction "Enter the following data".
- Three input fields for "Frequency slip limit((in HZ)", "VMag limit((in pu)", and "Vphase Angle limit((in deg)".
- A "LAUNCH" button.

**Fig 3.7:** Initial form of the Input screen window

The different channel IDs selected by the user can be chosen from the list in the dropdown menu which populates according to the type of measurements selected from the “openECA.db” database, stored in the user’s system. Once the appropriate measurement channel’s signal reference IDs are entered into the analytic by pressing the ENTER button, the following method is invoked, and a

thread is started to execute the main window application of openECA creating an openECA framework.

```
private static void ThreadStart_for_main_window()
{
    Algorithm.UpdateSystemSettings();
    Framework framework = FrameworkFactory.Create();
    Algorithm.API = new Hub(framework);
    MainWindow mainWindow = new MainWindow(framework);
    mainWindow.Text = "C# PMU_Synchroscope Analytic";
    Application.Run(mainWindow);
}
```

**Fig 3.8:** Code structure for creation of openECA framework

This particular action maps the respective measurement channel data to the respective data structures by creating a “UserDefinedMapping.ecamap” file (Figure 3.11). It utilizes the respective Historian ID (highlighted in the blue box) of the signal reference IDs (highlighted in red box), chosen by the user from the “Active Measurement Table” inside the database (Figure 3.10) and creates a JSON script as depicted in the following figures.

```
// Add new mappings to the MappingWriter
// and write the results to a file
MappingWriter writer = new MappingWriter();
writer.Mappings.Add(input_map);
writer.Mappings.Add(output_map);
writer.Write(Path.GetFullPath("Model\\UserDefinedMappings.ecamap"));
```

**Fig 3.9:** Code Structure for creation of the mapping file

openECA.db

File Edit Database GoTo Script Window Help

Design Data SQL Verify Analyze Chart Vacuum Log Settings

	Nod...	Sour...	ID	Sign...	Poin...	Alter...	SignalReference	Inter...
Protocol	e57b4...	e57b4...	PPA:1	a0655...	TVA_T...	NULL	TESTDEVICE-SF	1
Runtime	e57b4...	e57b4...	PPA:2	c19dd...	TVA_T...	NULL	TESTDEVICE-FQ	1
SecurityGroup	e57b4...	e57b4...	PPA:3	e49c8...	TVA_T...	NULL	TESTDEVICE-DV1	1
SecurityGroupUserAccount	e57b4...	e57b4...	PPA:4	5694a...	TVA_T...	NULL	TESTDEVICE-DF	1
SignalType	e57b4...	e57b4...	PPA:5	aaada...	TVA_T...	NULL	TESTDEVICE-PM1	1
Statistic	e57b4...	e57b4...	PPA:6	dc987...	TVA_T...	NULL	TESTDEVICE-PA1	1
Subscriber	e57b4...	e57b4...	PPA:7	a7609...	TVA_T...	NULL	TESTDEVICE-PM2	1
SubscriberMeasurement	e57b4...	e57b4...	PPA:8	32d4...	TVA_T...	NULL	TESTDEVICE-PA2	1
SubscriberMeasurementGroup	e57b4...	e57b4...	PPA:9	3e530...	TVA_T...	NULL	TESTDEVICE-PM3	1
TrackedChange	e57b4...	e57b4...	PPA:10	6ff25...	TVA_T...	NULL	TESTDEVICE-PA3	1
UserAccount	e57b4...	e57b4...	PPA:11	f6a84...	TVA_T...	NULL	TESTDEVICE-PM4	1
Vendor	e57b4...	e57b4...	PPA:12	b427...	TVA_T...	NULL	TESTDEVICE-PA4	1
VendorDevice	e57b4...	e57b4...	PPA:13	12f48...	TVA_T...	NULL	TESTDEVICE-PM5	1
SYSTEM	e57b4...	e57b4...	PPA:14	13e3f...	TVA_T...	NULL	TESTDEVICE-PA5	1
VIEWS	e57b4...	e57b4...	PPA:15	96a36...	TVA_T...	NULL	TESTDEVICE!PMU-ST1	1
ActiveMeasurement	e57b4...	e57b4...	STAT:16	51a8f...	TVA_T...	NULL	TESTDEVICE!PMU-ST2	1
AppRoleSecurityGroupDetail	e57b4...	e57b4...	STAT:17	9aa94...	TVA_T...	NULL	TESTDEVICE!PMU-ST3	1
AppRoleUserAccountDetail	e57b4...	e57b4...	STAT:18	c1398...	TVA_T...	NULL	TESTDEVICE!PMU-ST4	1
CalculatedMeasurementDetail	e57b4...	e57b4...	STAT:19	e30ae...	TVA_T...	NULL	TESTDEVICE!PMU-ST5	1
CurrentAlarmState	e57b4...	e57b4...	STAT:19	e30ae...	TVA_T...	NULL	TESTDEVICE!PMU-ST5	1

**Fig 3.10:** Active measurement Table containing the historian IDs and signal reference IDs

```

GPA test_DataIn Map_in {
  test_VoltMag1: PPA:81
  test_VoltAng1: PPA:80
  test_VoltMag2: PPA:82
  test_VoltAng2: PPA:8
  test_Incoming_freq: PPA:83
  test_Reference_freq: PPA:84
  Roc_incoming_phasor: PPA:85
  Roc_Reference_phasor: PPA:86
  test_CB_status: PPA:87
}

GPA test_DataOut Map_Out {
  CB_close: PPA:78
  CB_open: PPA:79
}

```

**Fig 3.11:** JSON script depicting the I/P and O/P data mappings

Thus, the link between the openECA and the analytic application in the form of an openECA framework has been created. Thereafter, the user can provide specific custom tolerance limits

depending upon system conditions and utility-specific design considerations. Special considerations have been taken into account to prevent errors on user behalfs such as invalid entries and blank entries, which would prompt the user with an error message.

### 3.2.3.2 Synchroscope Form Window

The display of the mockup analytic is designed with consideration to have better representation for the user encompassing all the features in a conventional synchroscope in addition to some new features. It includes real-time graphical plots for the incoming and reference voltage measurements and frequency measurements along with total downstream delays and the advanced angle depiction boxes as shown in the figure 3.12.

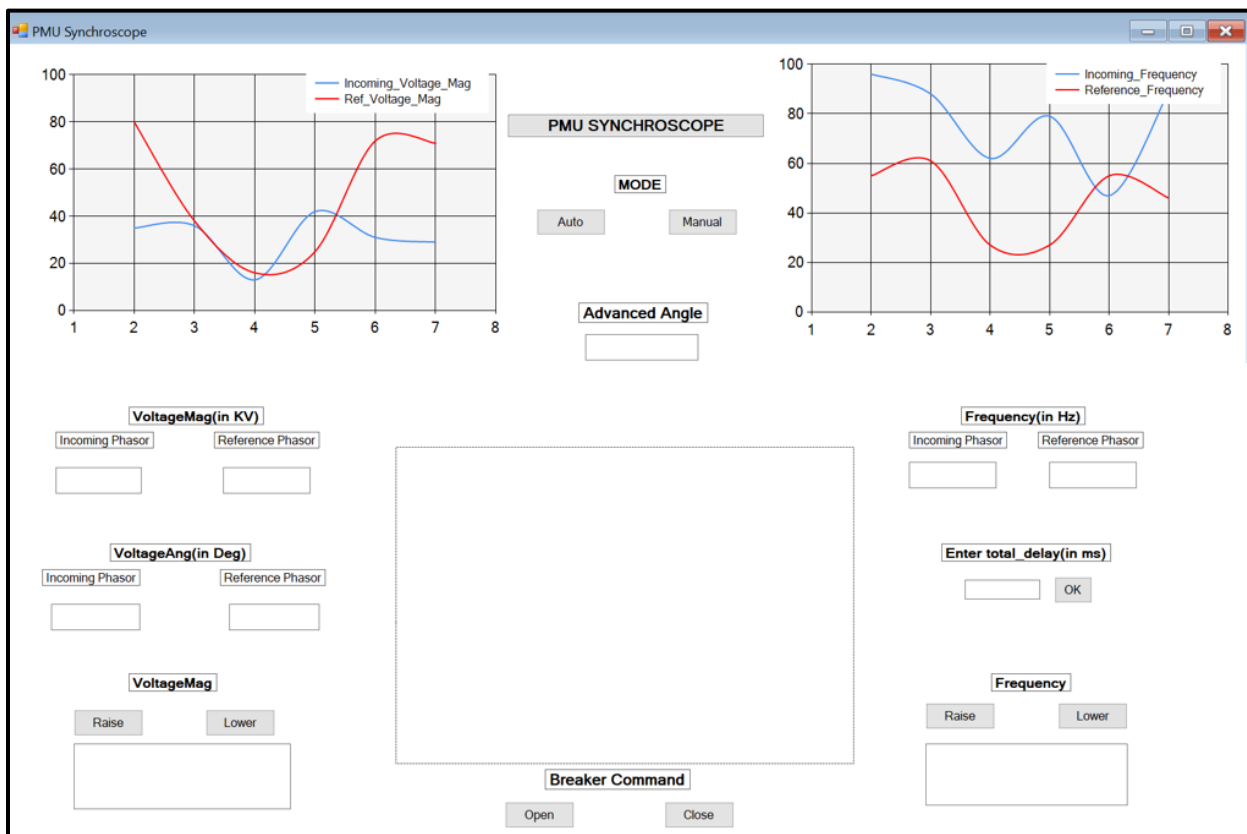


**Fig 3.12:** Initial form of the Synchroscope form window

This synchroscope form is continuously updated invoking the “Update\_measurements” method as depicted below which outputs the breaker close or open command signal in each frame (which is same as the frame rate of retrieval of PMU measurements from the openECA platform).

```

//Receive current updated frame of measurements and use it to generate the o/p measurements
public void Update_measurements(out bool CB_close, out bool CB_open)
{
    [Assign data to variables]

    [breaker buttons indication]

    [Textbox values Updation]

    [ Alarm boxes]

    [ Start the graphs once data starts streaming in]

    TimeIntervalupdate();           //call this function to update time interval for smooth transition
                                   //for depiction between two frames

    CB_close = breaker_close_command;           //return breaker Commands
    CB_open = breaker_open_command;
}

```

**Fig 3.13:** Code structure for Update\_measurements method

The angular position of the rotating phasor hand inside the synchroscope form is updated based upon the angular difference of the incoming voltage phase angle with respect to the reference voltage phase angle which is subjected to the frame rate of retrieval of data from the openECA platform (usually 30 frames per sec). However, the frame retrieval time can amount to a lower value depending upon the system. To have a smooth transition between updating the synchroscope form for a low retrieval frame rate case, a method named “TimeIntervalupdate” is invoked, which retrieves the frequency slip in the current frame and would update the phasor hand to a predicted value of angular difference position until the next frame is received. This prediction is made based upon principle as described in equation (1) in chapter 2, under the assumption that no significant changes would have occurred in the system until the next frame is received. If the frequency has changed, then the actual position of the phasor hand based upon the new phase angle difference

and the predicted position might change, but as the frequency doesn't drastically change and the frame rate is normally 30 fps, the analytic developed produces a much reliable prediction.

```
//Update the time interval to be used between two consecutive frames
public void TimeIntervalupdate()
{
    if (Math.Abs(Ref_Phazor_Frequency - Incoming_Phazor_Frequency) < (1000/360))//t.interval should be > 1 ms
    {
        if (Math.Abs(Ref_Phazor_Frequency - Incoming_Phazor_Frequency) < 0.01)
        {
            t.Interval = 277; //if slip is very minimal(<0.01 Hz) we assign a significantly large value to
            //make the phasormag hand stop because following the formula gives t.Interval
            //is nearly equal to infinity .
        }
        else
        {
            t.Interval = Convert.ToInt32(1000 / (360 * Math.Abs(Ref_Phazor_Frequency - Incoming_Phazor_Frequency)));
        }
    }
    else
    {
        t.Interval = 1;
    }
    if (t.Interval >= Convert.ToInt32(refresh_time))
    {
        t.Interval = Convert.ToInt32(refresh_time); //Use refresh time as image should be refreshed within
        //this time period at max.
    }
}
}
```

**Fig 3.14:** Code structure for TimeIntervalupdate method

Hence, the standalone PMU synchroscope project is created and executed to check for errors. Finally, an executable application file (.exe file) for the application is created using the “PMU\_Synchroscope” setup project file created by openECA (the file can be viewed on GITHUB site). The developer can customize the installation package file as per his/her specifications. Once the .exe file is created, it can be installed and viewed under the “GridProtectionAlliance” folder in the installed directory. Hereafter, the focus is to build an implementation platform for its validation and closed-loop control functionality. This was a carried out in a two-fold process as discussed in the following sections.

### 3.2.4 Test setup using RTDS simulated data using CSV adapter

For the initial validation and proper depiction of the basic functionalities of the application, the analytic was to be tested with the data generated by RTDS (Real-time Digital Simulator) at Dominion Energy, Richmond. A predefined blackstart model was executed on the RTDS platform and the synchronization data of the two buses to be synchronized, before and after synchronization were recorded. The data was collected in the form of a .csv file and later modified to replicate as simulated PMUs. In order to achieve that, proper measurement channels for the desired PMUs are first manually created inside the openECA manager as shown below in figure 3.15.

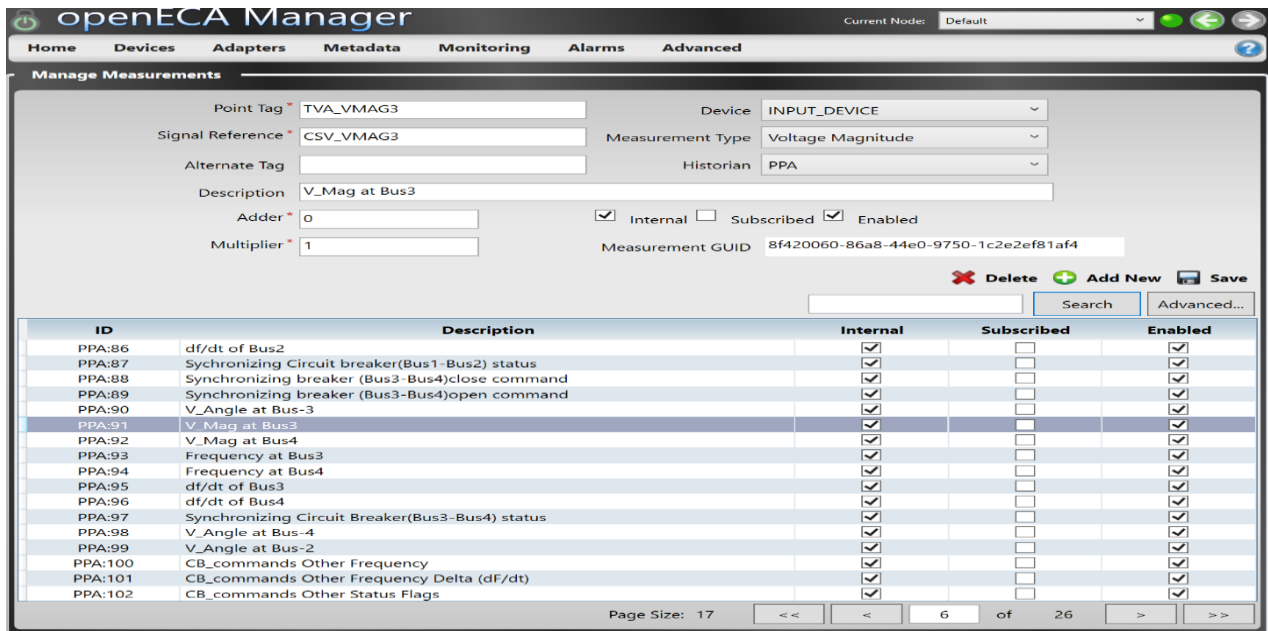


**Fig 3.15:** Creation of measurement channels for simulated PMUs

Thereafter, using csv input adapter functionality in the openECA manager, the appropriate column data in the csv files are mapped to the respective measurement channels using the historian IDs as highlighted below, thus generating the two simulated bus PMUs.

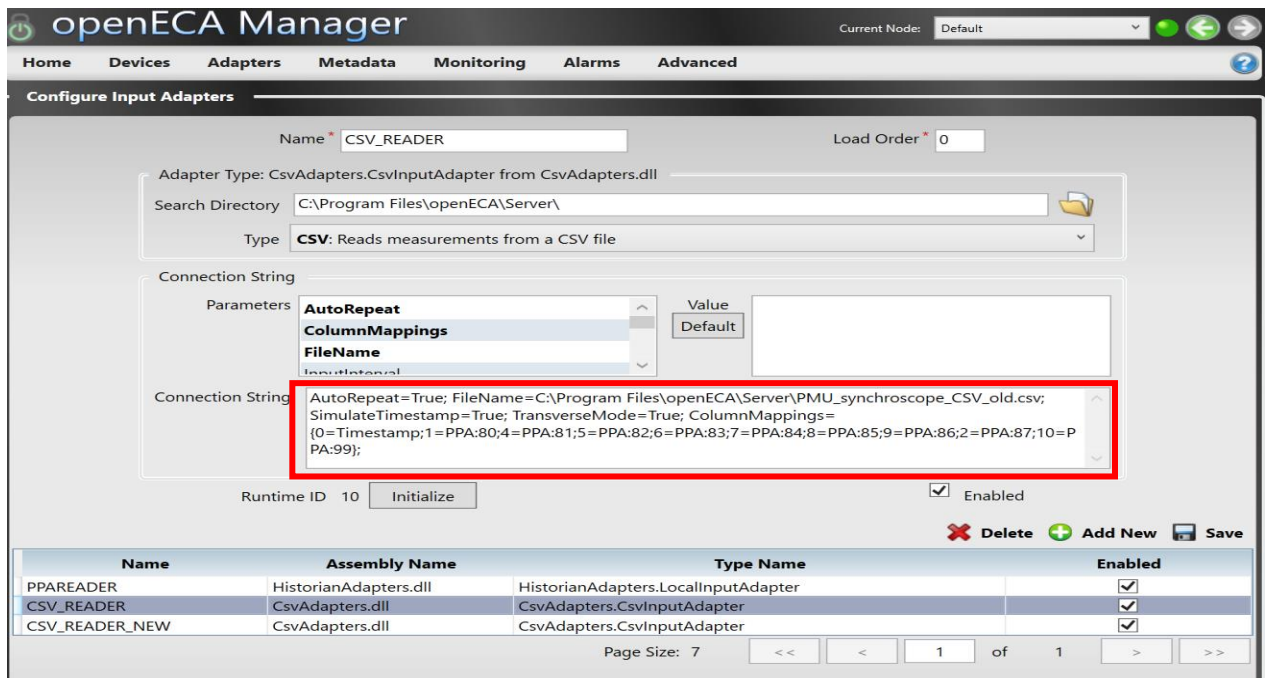


**Fig 3.16:** Using csv adapter to generate simulated PMUs

The observations after the execution of the RTDS simulated data are explained in detail in the next chapter.

### 3.2.5 Test setup using OPAL-RT ePHASORSIM simulator

The RTDS simulated data was a test for validation and proper depiction of using openECA platform with the developed analytic, but it did not encompass a closed loop control where the user can initiate breaker command signals back to the openECA platform or any power system model. To achieve this functionality, Dominion Energy procured an ePHASORSIM digital phasor simulator manufactured by OPAL-RT technologies for the project. ePHASORSIM is a tool for projects that involve dynamic simulation of power systems and is used for the testing and integration of EMS/SCADA systems, wide area protection, and control schemes, training and power system studies and simulations in real time. ePHASORSIM's phasor domain solver, performing at a typical time-step of few milliseconds, provides voltage and current information

representing the same as phasor measurement unit (PMU) installed in the power grid [22]. This unique electromechanical real-time simulation system enables precise simulation of large-scale networks within a real-time and faster performance. ePHASORSIM real-time simulation is performed under the OPAL-RT's flagship RT-LAB simulation platform. It allows ePHASORSIM to be connected as part of a larger Simulink model, enabling researchers to benefit from a complete grid ecosystem, as well as having access to all OPAL-RT hardware modules and I/O and communication protocols such as DNP3, OPC-UA, C37.118 and interconnect the real-time simulation with physical devices under test [22]. The platform also offers all features for monitoring, data processing and data acquisition to facilitate testing, analysis, and reporting. A collection of models for the positive sequence as well as three-phase unbalanced power grids is provided in a library of ePHASORSIM. The library includes models of generators and their controllers, loads, transformers, current injector devices and voltage sources, along with various types of events associated with each component to simulate complex operating and control scenarios in real-time. For the synchroscope application, the inbuilt models provided by ePHASORSIM have been used as a benchmark model with modifications.

The closed-loop feedback functionality of the PMU synchroscope can be demonstrated with the help of the creation of a two islanded model system, and the measurements of the two buses to be synchronized emulated as two separate PMU measurements. For demonstration purpose, real-time simulated PMU data are streamed in using the OPAL-RT ePHASORSIM simulator. A custom modified two islanded model for the 39 bus IEEE system is generated and executed on the target simulator. The PMU Synchroscope is installed on the same desktop PC as openECA and establishes a connection with openECA over GEP (Gateway Exchange Protocol) for input and output measurements. Figure 3.17 depicts the information flow diagram of the test setup.

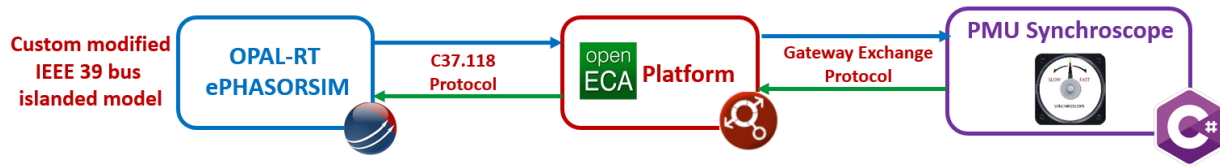


**Fig 3.17:** Information flow diagram of the test bed setup

### 3.2.5.1 Custom modified IEEE 39 bus two-island model

This section discusses the RT-LAB software and setting up the procedure of the custom modified model. RT-LAB software requires MATLAB Simulink to run the models along with Simulink Coder for code generation to be used to finally load the model on the ePHASORSIM target simulator. Once the RT-LAB application is installed and executed, a new model can be created in its main tab as shown. ePHASORSIM provides with some inbuilt model templates as depicted in figure 3.18. The user can use them and modify as per their specifications if required.

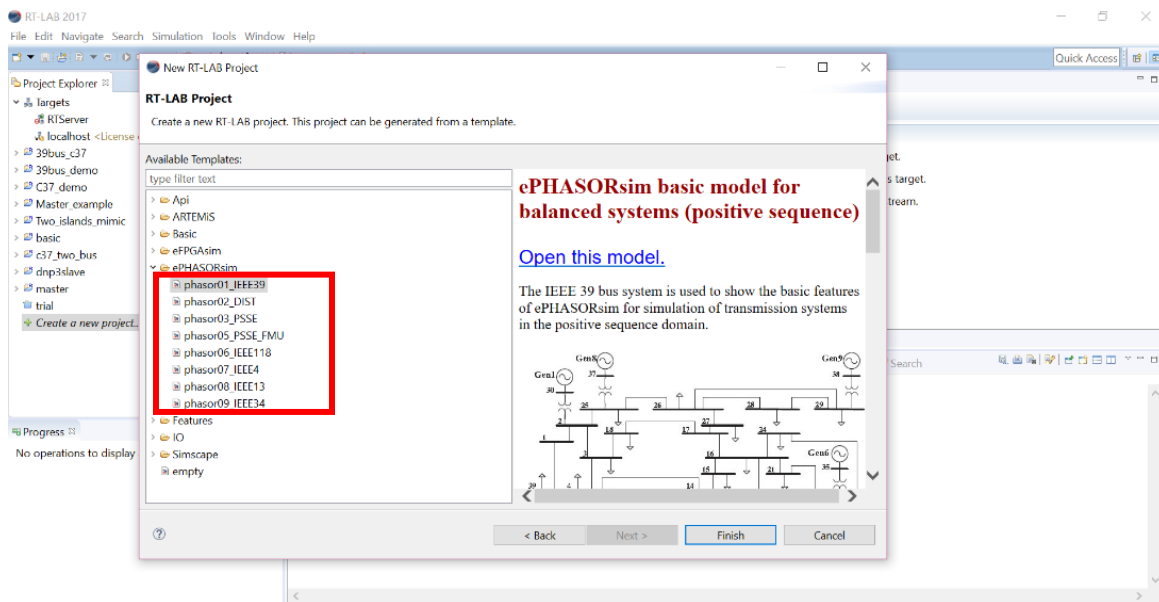


**Fig 3.18:** Inbuilt ePHASORSIM models for project startup.

For the sake of this project, a small yet relatively complex model of IEEE 39 bus system was taken into consideration and later modified to fit the requirements as explained later. The original IEEE 39 bus system model is represented in figure 3.19.

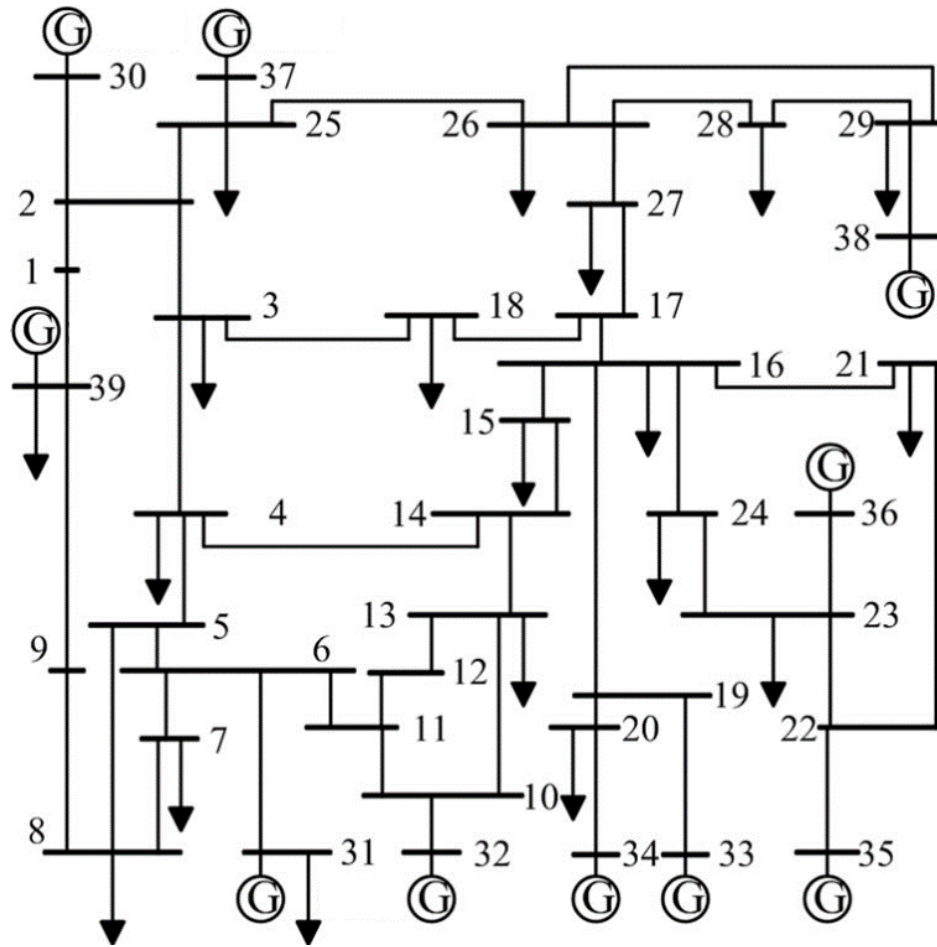


**Fig 3.19:** Original IEEE 39 bus system

Hereafter, to modify the original IEEE 39 bus model into a two-islanded system, lines connecting buses 3 to 4, 17 to 16 and 39 to 9 have been disconnected. Moreover, to represent a practical, realistic scenario an additional node 46, which is present in substation 39, was added to the system. Hence, to synchronize the two islands, the synchronizing breaker between bus 39 and bus 46 must be closed. Note that the nomenclature 46 is used as several other nodes were also introduced at substation 16 to be used for a “Substation Based Topology Estimation” analytic using the same model as a part of the same openECA project.

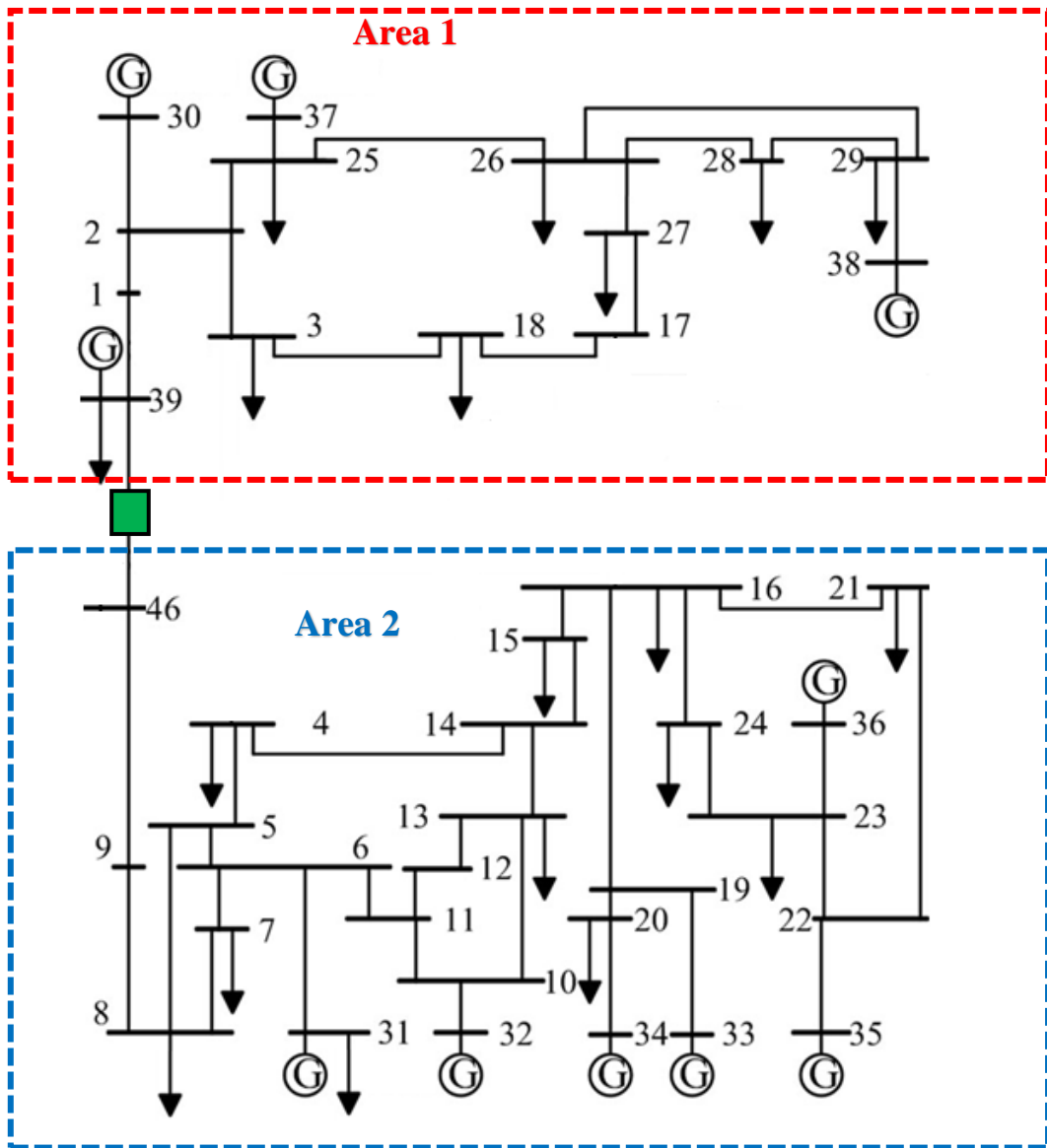


**Fig 3.20:** Custom modified IEEE 39 bus two-islanded model

Now to create the Simulink model and to generate the simulated PMUs, the C37.118 slave example model inside RT-LAB database is used as a benchmark model. This includes a computational block (represented as a `sm_pmu_37_118` block) and graphical user interface block (`sc_console` block) as depicted in the figure 3.21. During real-time simulations, the user can only control any inputs or parameters provided in the console block whereas the computational block is primarily focused on the background computational activities such as the power flows and dynamic simulations required.

Notes

- In this model, the IEEE 39 bus system model has been custom modified to represent a two islanded system with Bus-16 modelled as a substation having additional nodes for showcasing the functionality of Substation Topology Estimator and PMU Synchroscope analytic for openECA project
- It operates at a nominal frequency of 60 Hz and the data rate can be chosen among a list of pre-defined rates or can be manually set as a custom data rate
- Signals in and out of the model are communicated over C37.118 protocol.

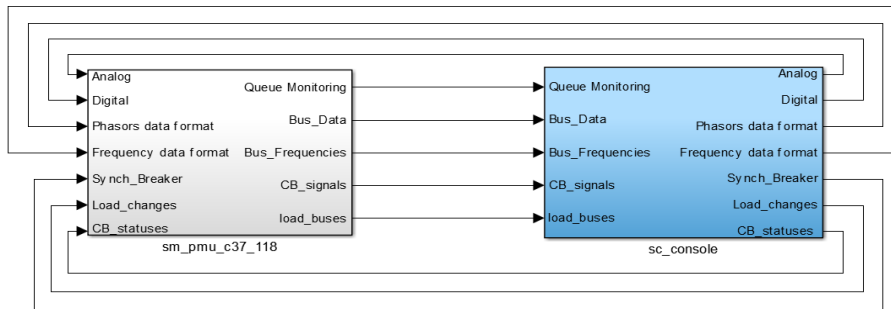


Fig 3.21: C37.118 Simulink model main window

### 3.2.5.2 Computational Block

In order to create a new ePHASORSIM model, RT-LAB/Phasor is selected from the Simulink library browser window, the ‘Solver’ block is dragged into the computational subsystem of a new Simulink model window.

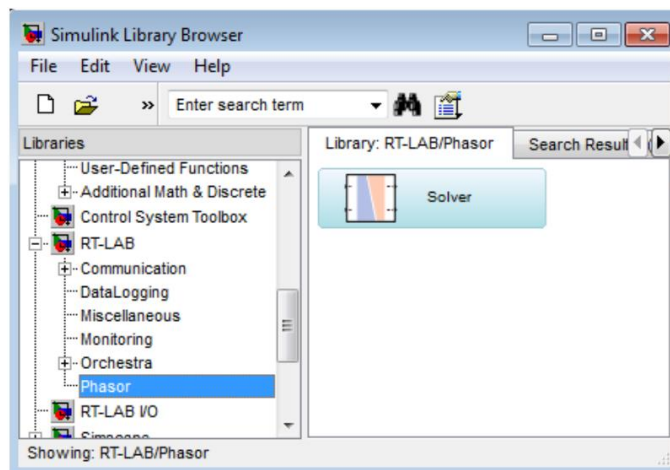
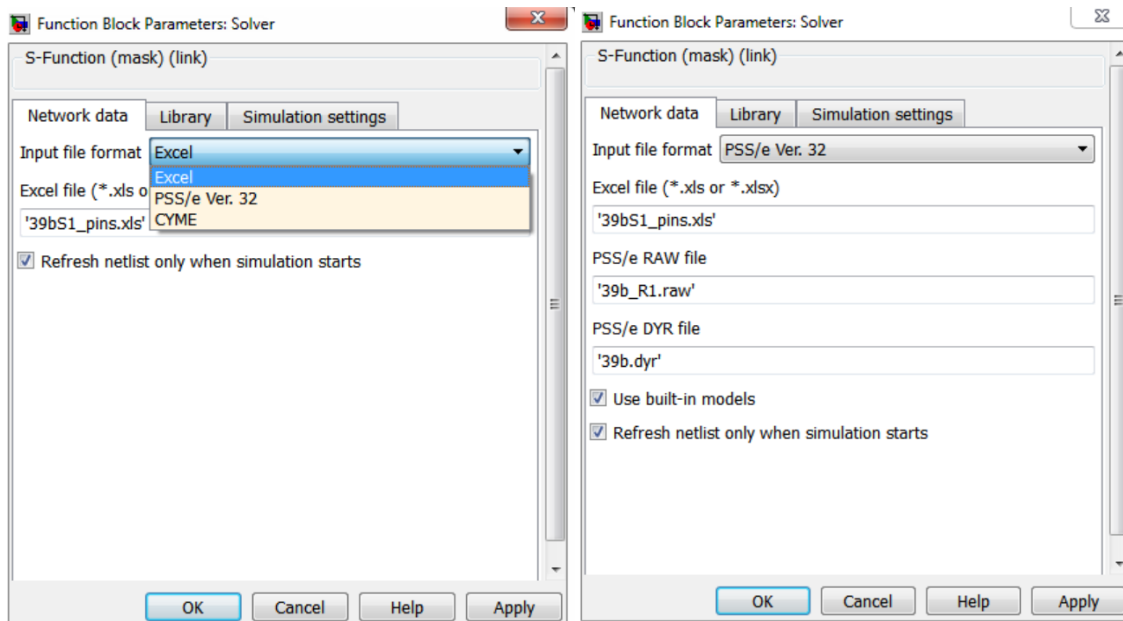


Fig 3.22: Solver Block (ePHASORSIM product)

Now the user can provide the input data and model parameters in three different formats inside the solver block mask. The user can choose between Excel, PSS/e Ver. 32, and CYME data entry

types. Each input format has distinct configurable parameters. The following figure shows the ‘Solver’ block mask configured for PSS/e input (Version 32).



**Fig 3.23:** Solver function Input file settings

If the PSS/e Ver. 32 input format is selected, only the ‘Pins’ page is required in the Excel input file. Additionally, the following format-distinct items need to be configured, as follows.

**The Pins file:** It is an excel file which denotes the incoming and outgoing pins for the solver block.

There are two types of pins:

- Outgoing: To define measurement probes or monitor a status in the power system (e.g. the voltage of a bus, or in-service status of a shunt device)
- Incoming: To send operational commands to the simulator (e.g. apply faults)

**PSS/e RAW file:** PSS/e's load flow data (\*.raw).

**PSS/e DYR file:** PSS/e's dynamic data (\*.dyr).

The simulation settings inside the solver mask, as depicted in the figure 3.24 are used to configure the power-flow and dynamic simulation solvers.

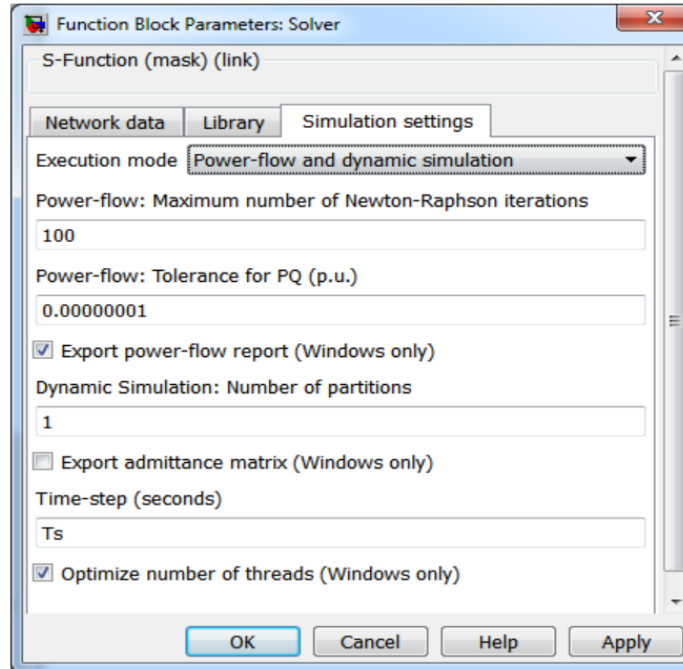


**Fig 3.24:** Simulation settings inside the Solver block

These settings specify the behavior of the ‘Solver’ block when the simulation is executed. For the purpose of the analytic, transients and dynamic behavior of the system after synchronization is required to be monitored and hence, the “Power-flow and dynamic simulation” mode is selected. In this particular execution mode, the solver block executes power-flow before running a dynamic simulation. The solver initializes dynamic components based on voltage and power values calculated by power-flow.

Now the Simulink model is created containing the solver block which contains the information for the power system model and is configured to emulate PMUs to act as a C37.118 slave model which can be loaded into the digital simulator as shown in figure 3.25.

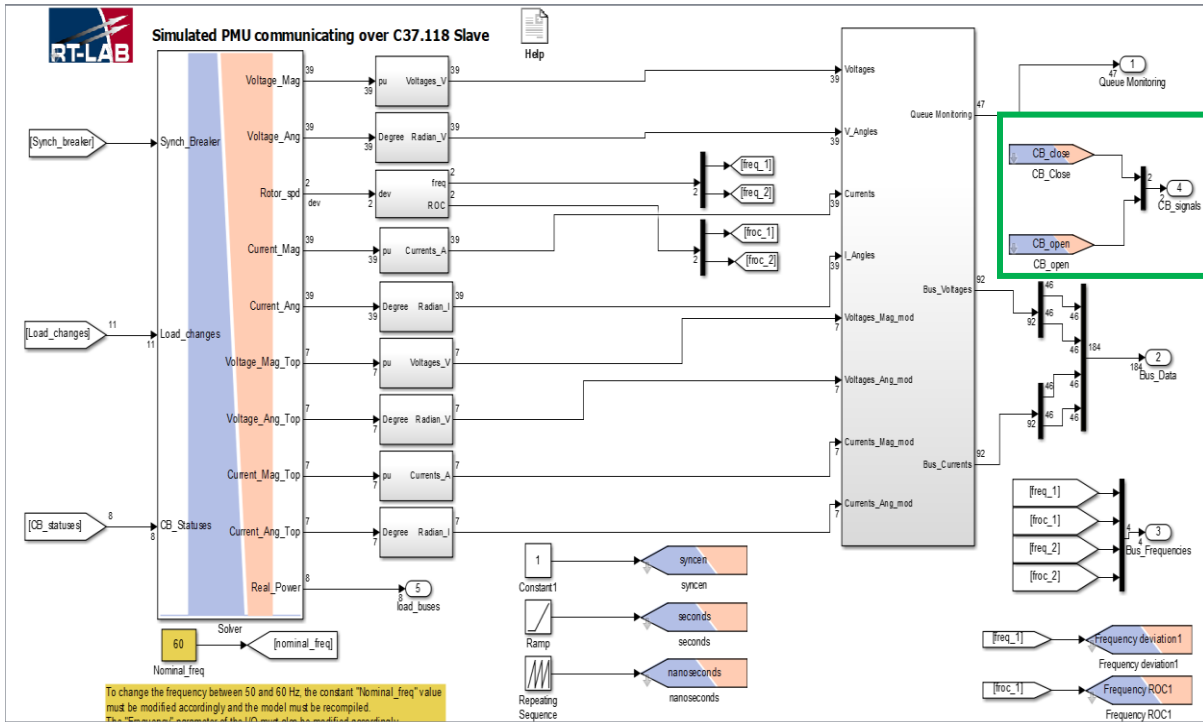


**Fig 3.25:** Computational subsystem Simulink model architecture

Apart from acting in a C37.118 slave configuration, the model has to be configured as a C37.118 master configuration in order to receive the breaker commands back from the openECA platform. This is achieved by incorporating the following two files along with the model.

1. **The master driver configuration file (.config)** which specifies the connection string for the target simulator to receive the signals from the user system.

```

OPAL-1.0 Object
C37118::Master::Configuration {
  autoRunAcq=1
  listeningTimeoutMs=30000
  specialAction=importCfg2
  specialAction=logToFile/error_tapas.log
  specialAction=exportConnect/connect_tapas.log
  specialAction=exportTree/c37118_master_driver_tapas.ptree
  pmuConnectionList {
    item {
      id=1
      ip=192.168.10.103
      port=4712
      protocol=TCP
      retryNbr=30
      alias=PMU-SYNCHROSCOPE
    }
  }
}

```

**Fig 3.26:** Master driver configuration file

2. The connection file (.opal), which specifies the mapping of the signals received with the respective input ports in the model which are highlighted in green in figure 3.25.

```

OPAL-1.0 Object
List<SyncExchangerConnections> {
  item {
    id {
      C37118Master
      configFile=c37118_master_driver.config
    }
    inputs {
      item {
        dataInExchanger=PMU_SYNCHROSCOPE/CLOSE.magnitude[0]
        dataInProcess=OpInput:CB_close[0]
      }
      item {
        dataInExchanger=PMU_SYNCHROSCOPE/OPEN.magnitude[0]
        dataInProcess=OpInput:CB_open[0]
      }
    }
  }
}

```

**Fig 3.27:** Master driver connection file

### 3.2.5.3 Console Block

The different real-time changes in the model parameters including closing the breaker close command as well as load changes can only be made inside this block. The following figure shows the model architecture inside the sc\_console block:

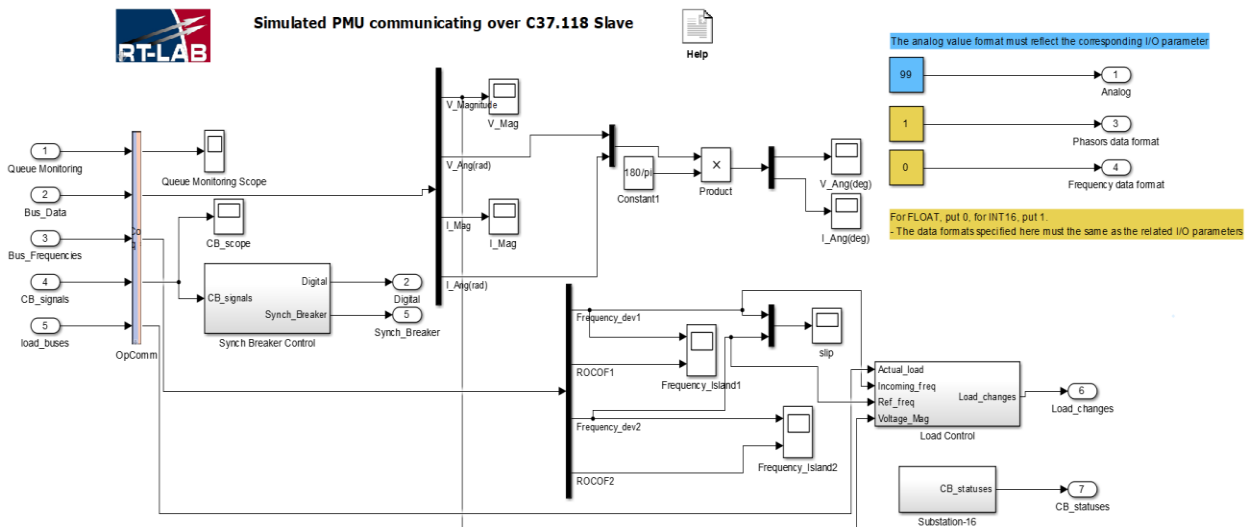


**Fig 3.28:** Model architecture of the console block

**The Synch Breaker Control block** receives the command initiated from the application via openECA platform and using the C37.118 master configuration driver of OPAL-RT as discussed earlier. It finally relays the breaker status back into the solver block of the main computational block as one of the incoming pins as seen in figure 3.25.

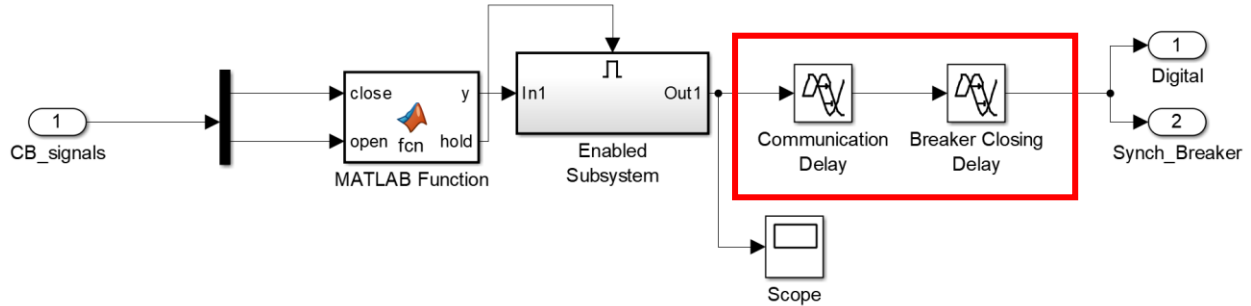


**Fig 3.29:** Synchronizing breaker control block

The highlighted region denotes the inclusion of delays in the system. It would represent both communication delays and breaker closing delays (otherwise represented as the downstream delays and termed constant as discussed earlier). Depending upon these delays, the breaker status would be changed in the model after the signal from openECA is received, thus emulating practical scenarios.

**The load control block** receives the frequency and voltage measurements, and the actual loads of the load buses inside the island to be controlled as the inputs. As discussed earlier, depending upon the slip in frequency and real-time voltage sensitivities calculations inside this block, the load changes to be made are displayed. The operator can thereafter manually change the load as stated in the algorithm specified earlier.

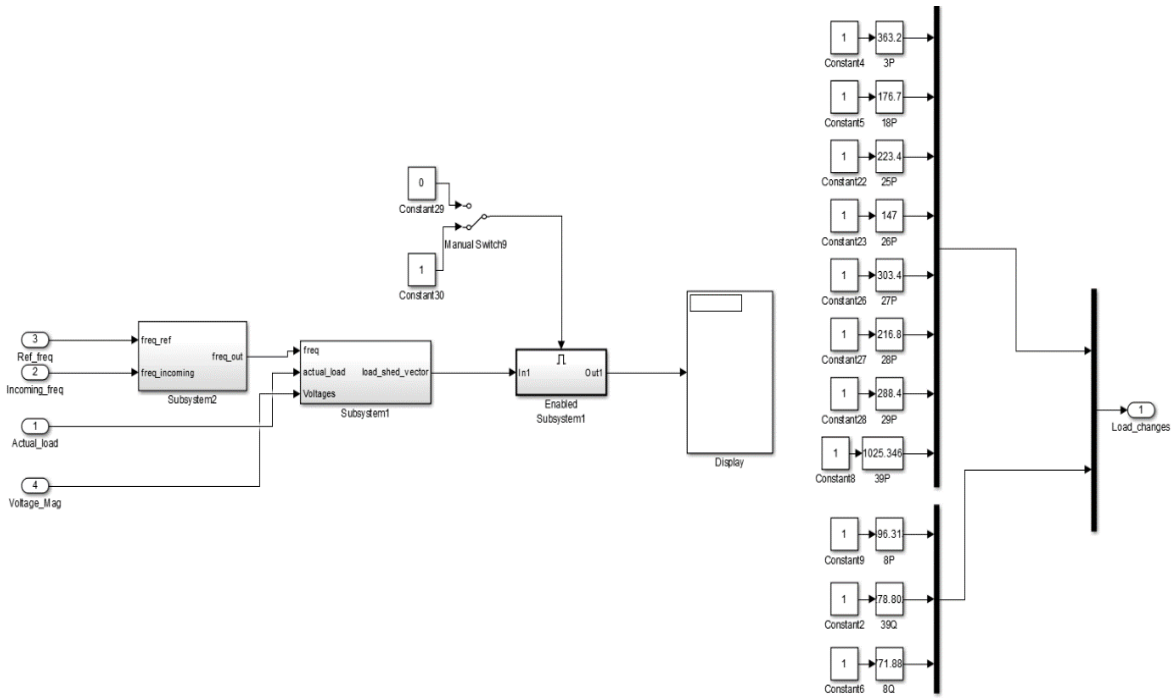


**Fig 3.30: Load control block**

### 3.2.5.4 Simulink Model configuration in RT-LAB

The Simulink model has been created, and the simulated PMU devices need to be created on the RT-LAB main window under the configuration section of the model, which would be streaming simulated PMU data over C37.118 protocol from the target simulator to the openECA platform.

**C37.118 Slave Configuration**

Associated subsystem: C37.118 Slave/sm\_pmu\_c37\_118

**General / Slaves / Bus1\_39sys**

Parameter	Value
ID	1
Protocol	TCP
TCP port	7201
NIC name	eth0
IP address	ANY
Frequency	60 Hz
Data rate	30 Per Second
Phasors representation	POLAR
Phasors format	FLOAT
Analogs format	INT16
Frequency format	FLOAT
Header	Default header

**Fig 3.31: Configuration of the simulated PMU devices**

The various specifications for the streaming of data along with the data format are provided for each simulated PMU device as shown in above figure. The next step is to connect the Simulink model parameters with the virtual PMU devices that have been instantiated as depicted in figure 3.32.

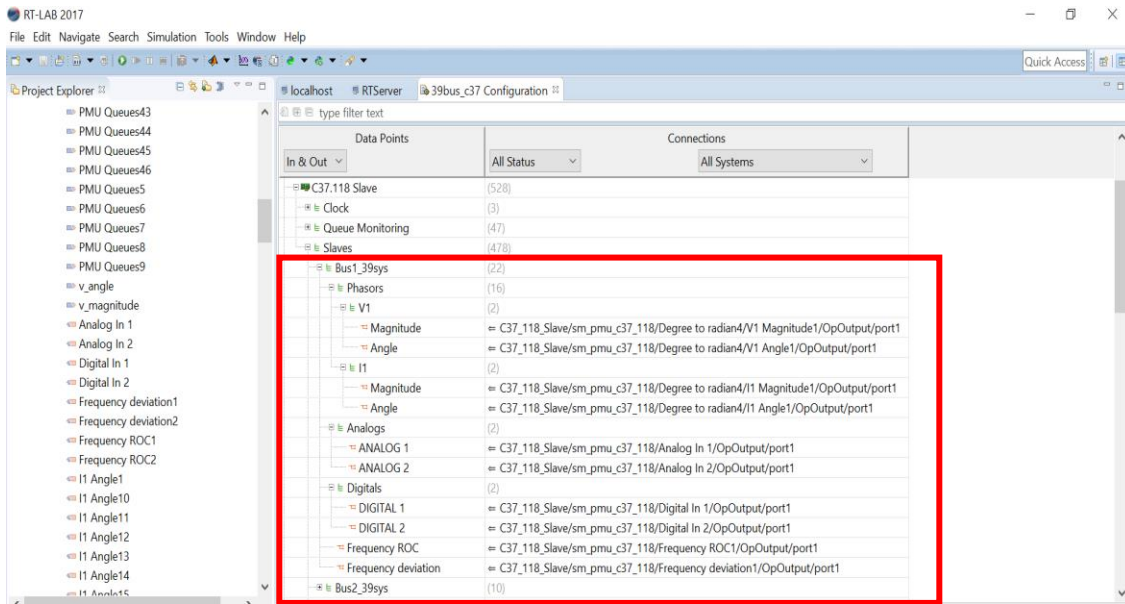


**Fig 3.32:** Configuration of the phasors of the simulated PMU devices

As can be seen from figure 3.31, the different PMUs have been created, and the input and output ports in the MATLAB Simulink model are mapped to the various measurements of any particular PMU device. Once all this mapping is done, the Simulink model is loaded and finally executed on the target simulator to stream real-time simulated data over C37.118 protocol.

### 3.2.6 Connection of the PMU devices to openECA platform

In this section, the procedure to retrieve the simulated stream of PMU data on the user system and the openECA instance is discussed. For adding these, the configuration and connection files of the respective PMU devices are required, which was collected using the “PMU Connection Tester” open source application. Using these configuration and connection files, the various PMU devices are then added to the openECA manager.

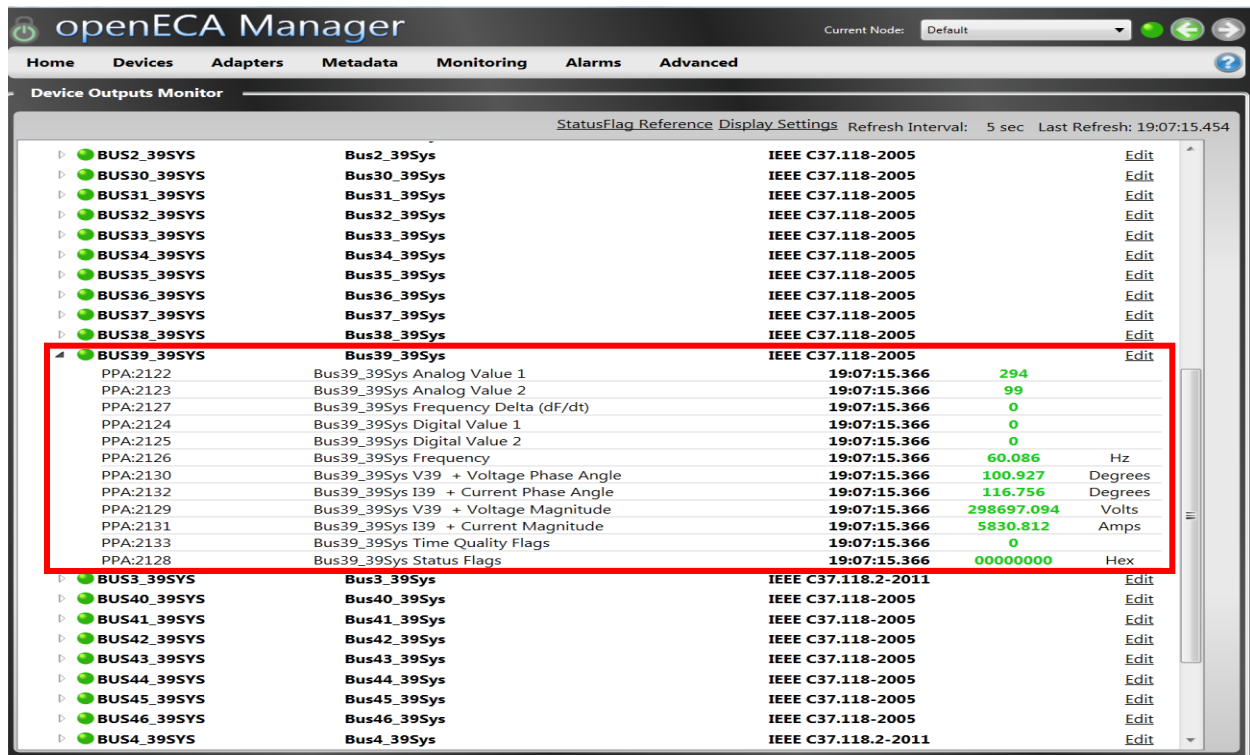


**Fig 3.33:** List of added PMU devices on the openECA platform

As depicted in the figure, the PMU devices show up in the device list, and if the model on the OPAL-RT LAB target simulator is up and running, then the healthiness of the stream of PMU data is indicated in green as depicted in figure 3.33. The various measurements of each PMU device can also be visualized as highlighted. Hence, the setup for including the simulated PMU devices to be later used in the synchroscope application is created and ready for use.

### 3.2.7 Configuring the output channels on the openECA platform

The final step is to set up the output adapters which would send the circuit breaker commands back to the simulator. This is achieved by setting up openECA in C37.118 slave configuration and configuring the concentrator output streams to stream data over C37.118 protocol under the concentrator output streams tab in the openECA manager application as depicted in figure 3.34.

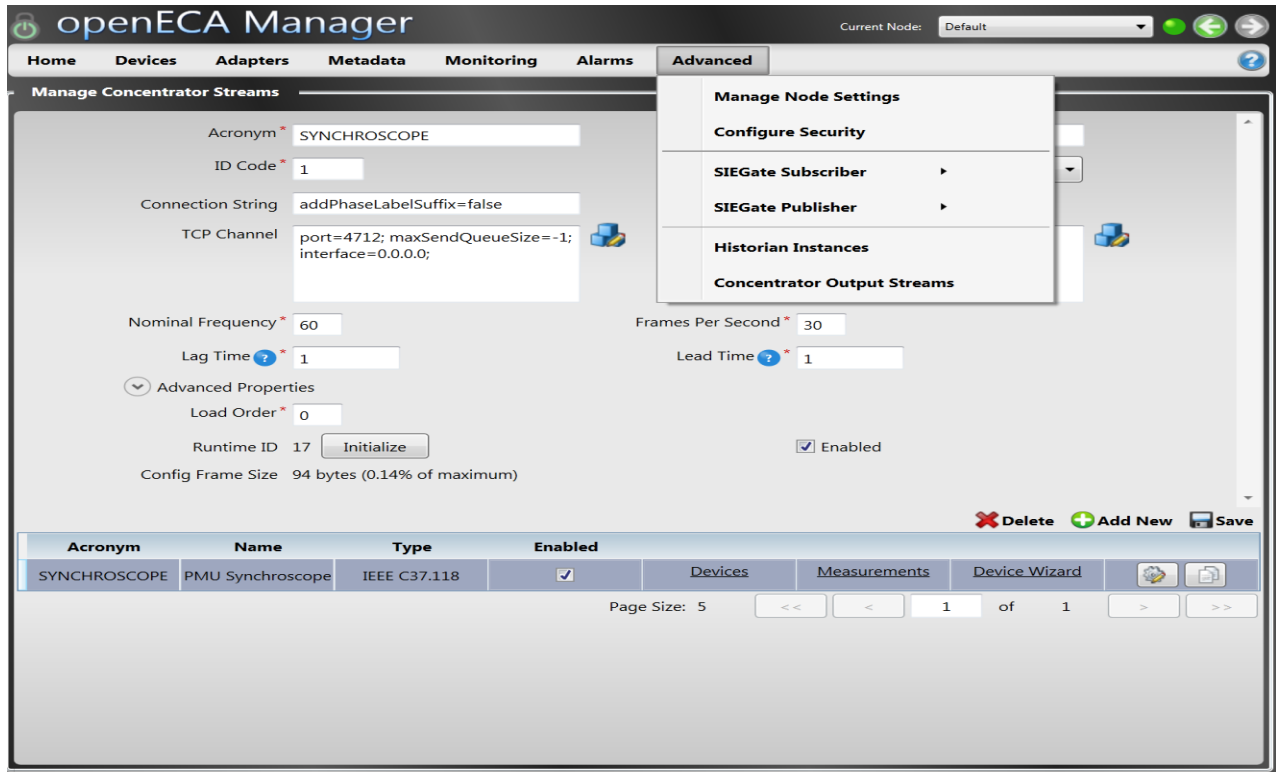


**Fig 3.34:** Configuring output streams for the breaker commands

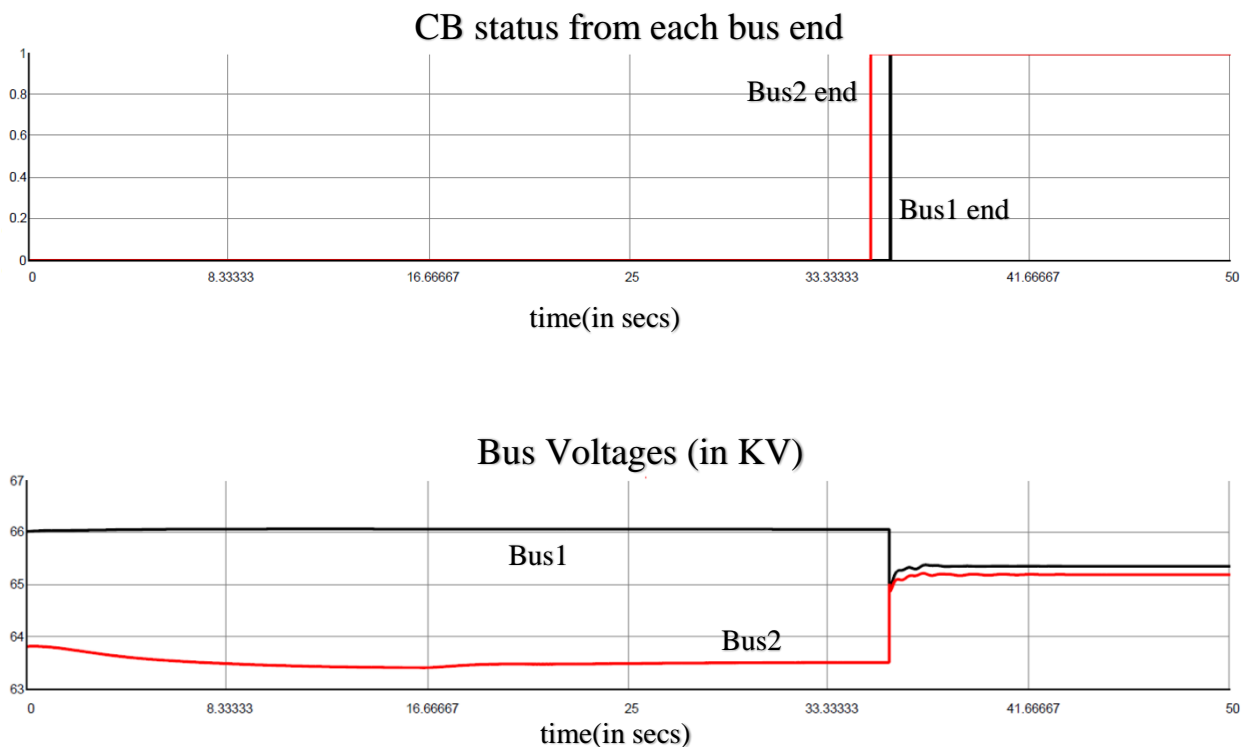
Hence, a close loop feedback starting with the designing of the application followed by the setting up of the simulator and its simulation settings to configuration of the simulated PMU devices on the openECA instance and finally sending the breaker command signals from the application via the openECA platform back to the simulator to modify the model parameters is established. This particular setup helped us to demonstrate the comprehensive functionality of the analytic in real time as discussed in the following chapter.

# Chapter 4: Test Scenarios and Results

This chapter would discuss the results, findings, and validation for the application developed in a two-fold approach as discussed earlier in the previous chapter.

## 4.1 Validation results using RTDS simulated data

Firstly, the application was tested using the RTDS simulated data provided by Dominion Energy, Richmond, using the predefined models available for their blackstart restoration procedure in order to validate the functionality of the application in its initial stages. The simulation was executed for 50 seconds, and the simulated data and plots were collected. The RTDS simulated data is provided in the appendix, and the plots for the same are depicted below in figure 4.1.



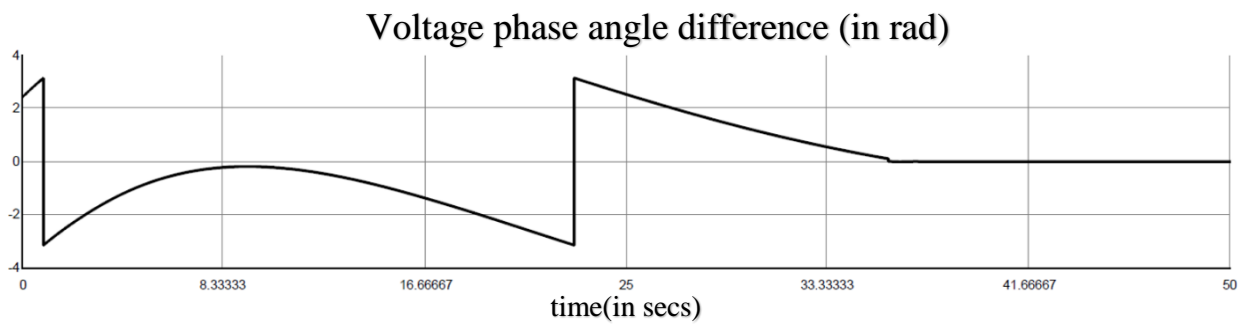
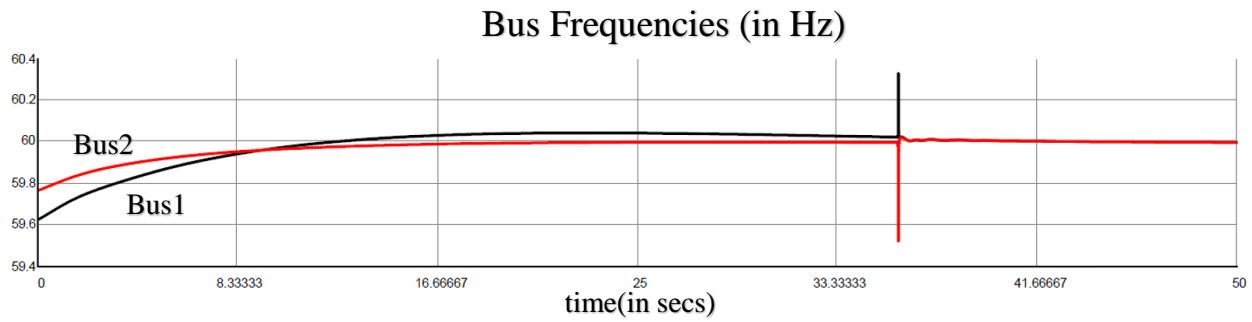


**Fig 4.1:** RTDS simulated data plots prior and post-synchronization

As depicted in the above figure, the system conditions were modified to have the frequency of the incoming island increase from below the reference frequency to finally surpass it. Thus, we have a variable slip scenario setup but without any close loop control feedback. The movement of the rotating phasor hand and the calculation of the advanced angle in order to correctly synchronize finally at minimal (ideally zero) degree phase angle difference was found to be in accordance to the data provided.

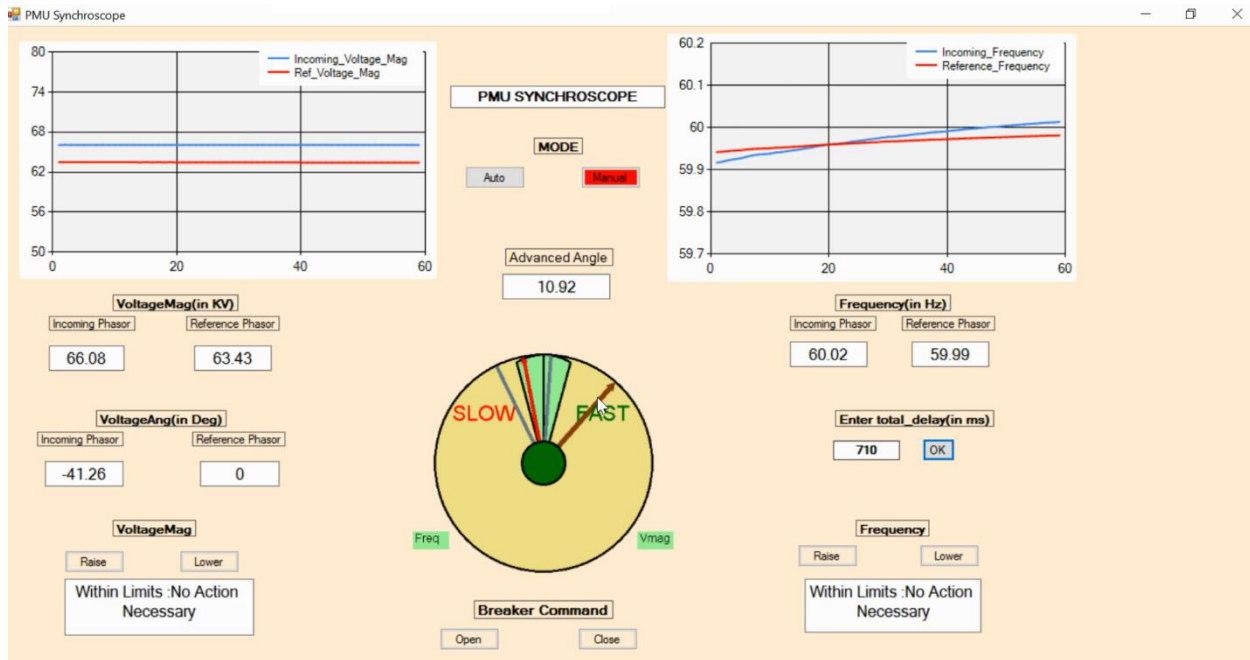


**Fig 4.2:** Synchroscope performance using RTDS simulated data

## 4.2 Testing results using OPAL-RT ePHASORSIM simulator

The previous exercise validated the generic functionality of the application. In the next stage, the closed-loop control feedback performance of the analytic is checked and therefore the necessary applications are installed on the respective systems to execute the modified two-islanded IEEE 39 bus model as discussed earlier.

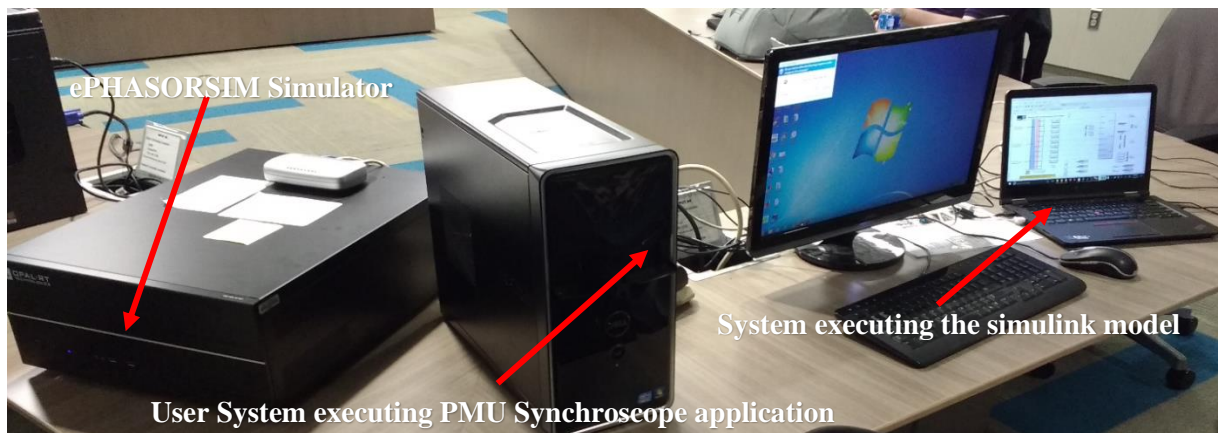


**Fig 4.3:** Test bench setup

Figure 4.3 displays the test bench setup for execution. The target simulator is loaded with the modified Simulink model and executed and streams PMU data over C37.118 protocol to the user's system, which would be controlling the PMU synchroscope application.

As discussed in the previous chapter, the various PMU devices have already been added on the openECA platform and thus as soon as the model is executed on the target simulator, real-time simulated data is received on the openECA platform which can be viewed in the "Trend Measurements" monitoring section as shown below.

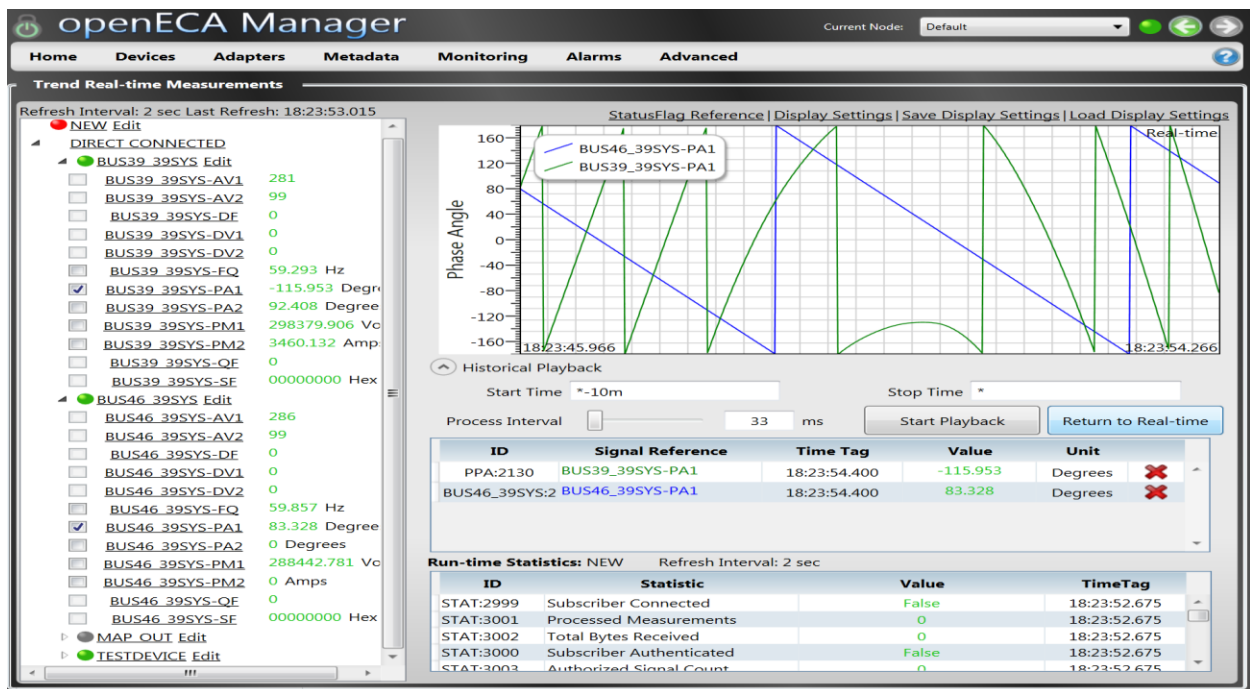


**Fig 4.4:** Trending real-time simulated measurements on openECA

As shown in the figure changing the loading conditions in the Simulink model, we have a variable frequency of the incoming phasor (Bus 39 in this case). The voltage phase angle in the above figure reverses its direction once the frequency of the incoming phasor crosses 60 Hz nominal frequency.

Hereafter, the PMU Synchroscope application file was installed on the user's system, and once it is executed, the user can then enter the various details as discussed earlier in the Input Screen

window, which would be populated in the drop-down menu collecting data from the openECA database as shown in the following figure.

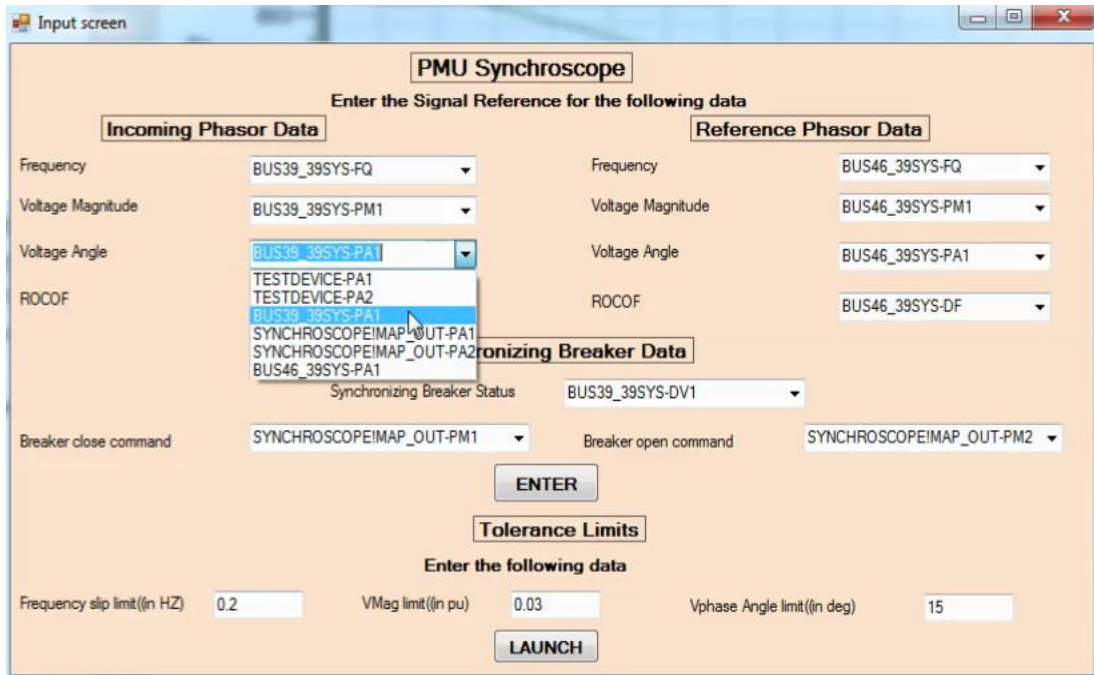


**Fig 4.5:** Input screen window

Once these details are entered, the openECA framework is created, and the respective data mapping is done, and finally, PMU data starts streaming into the application. The estimated mean frame rate received can be viewed in the concentrator section of the main window pop up once the framework is created. Apart from that, the upstream delays which are calculated based upon the total time difference of the input data time stamps and the Universal coordinated time (UTC) on the system are also displayed in the algorithm section of the main window pop up as specified in the code. In this particular case, the upstream delays are around 600 milliseconds as can be seen from the figure 4.6.

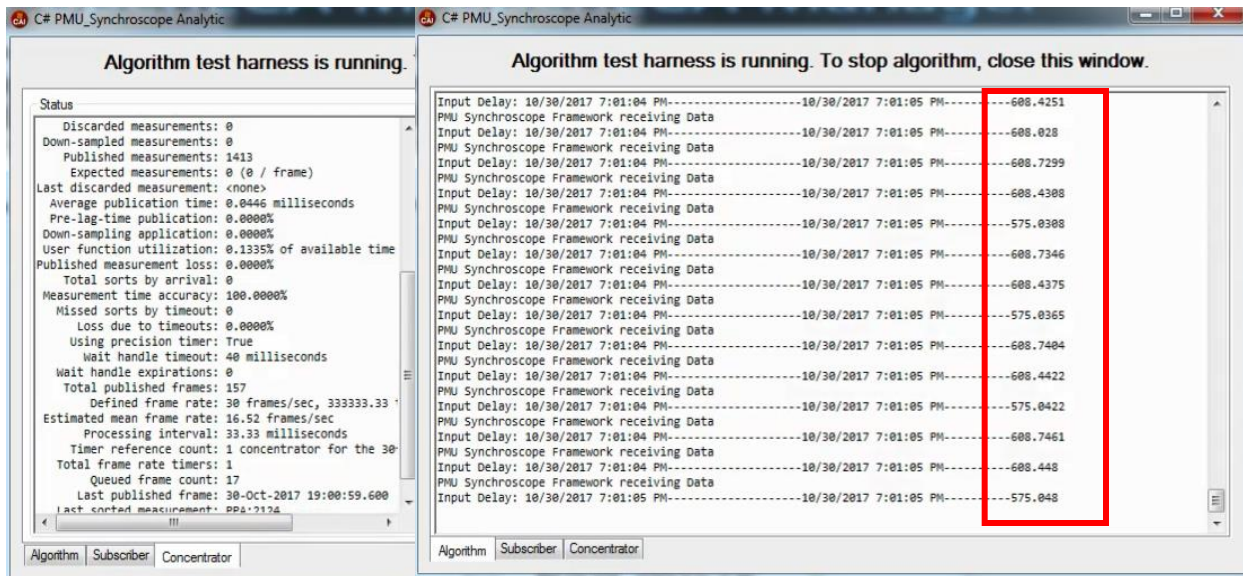


**Fig 4.6: Analytic Main Window**

Hereafter, the tolerance limits for successful synchronization which can be user/utility specific depending upon system conditions are provided, and the PMU synchroscope form window is finally launched as shown in the figure below.

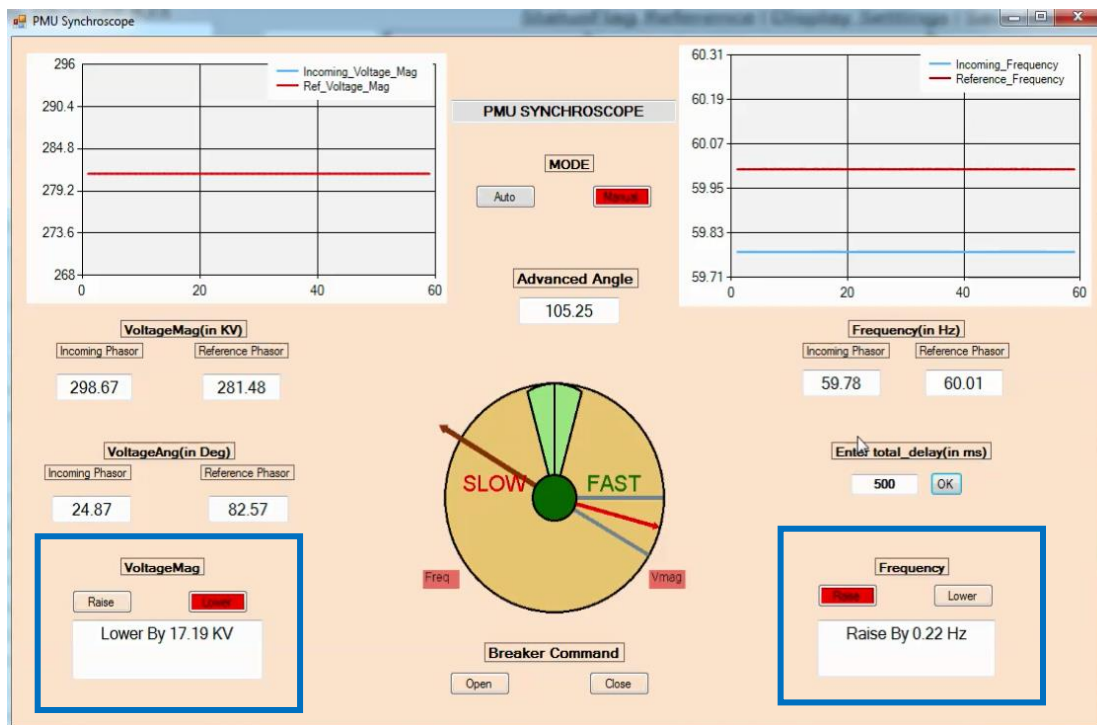


**Fig 4.7: Synchroscope Form Window prior synchronization**

A total downstream delay of 500 milliseconds is entered in this window and depending upon the slip in frequency between the two buses, an advanced angle is calculated and displayed as shown in the figure. The center of the synchroscope form depicts the breaker status, which is green in the above figure denoting that the synchronizing breaker between Bus-39 and Bus-46 is open. As we can see as the difference in the various measurements are out of the tolerance limits, proper annunciations and respective actions are displayed highlighted in the blue boxes, and therefore, the checklist indicates that the breaker close command cannot be initiated. Once respective actions are carried out by the operator and the measurements across both sides of the synchronizing breaker are brought within respective tolerance limits, the breaker close command can either be initiated manually in “Manual” mode or automatically sensed by the application at the advanced angle position in the “Auto” mode.

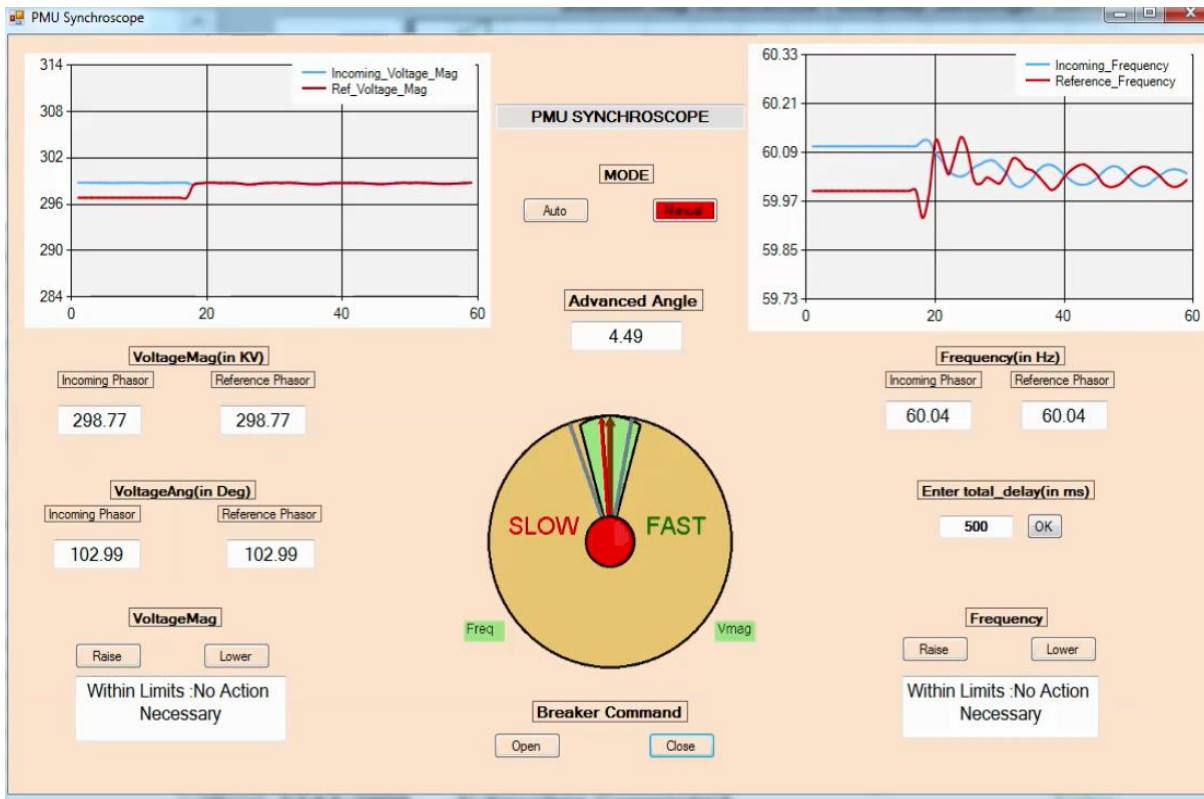


**Fig 4.8:** Synchroscope Form Window post synchronization

It can be observed from figure 4.8, that the transients after the synchronization are acceptable and dies out after some interval, thus leading to proper and successful synchronization.

As discussed earlier, the synchroscope application would only raise annunciations communicating to the user how much change in the measurements needs to be achieved. But it doesn't direct the procedure how to achieve it and thus, the following section discusses the performance of the load control technique using voltage sensitivities of the load buses of only one island which is to be controlled (in this case the incoming island which is Area -1) as discussed in the earlier chapters . This technique also helps to reduce the after synchronization transients as the slip between the two islands is reduced to a minimal value. Two scenarios are considered to depict the load control technique functionality and how the operator might utilize this for controlling the frequency of the island.

1. The incoming phasor frequency is higher than the reference phasor frequency.
2. The incoming phasor frequency is lower than the reference phasor frequency.

### **Scenario-1:**

In both the scenarios, the loading in area-2 (Reference island) is modified to maintain a reference phasor frequency of 60.01 Hz. Now modifying the system conditions and maintaining the loading conditions as depicted below in the table, the frequency of Area-1 is brought to **60.19** Hz. The following table depicts the loads at the various PQ buses in Area-1.

Bus Number	Load (in MW)
3	356.6
18	172
25	217
26	140

27	296
28	206
29	282
39	919.355

**Table 4.1:** Loads at various PQ buses of Area-1 prior load control (Scenario-1)

The voltage phase angle profile of the two islands with such a large slip can be visualized from the following figure.

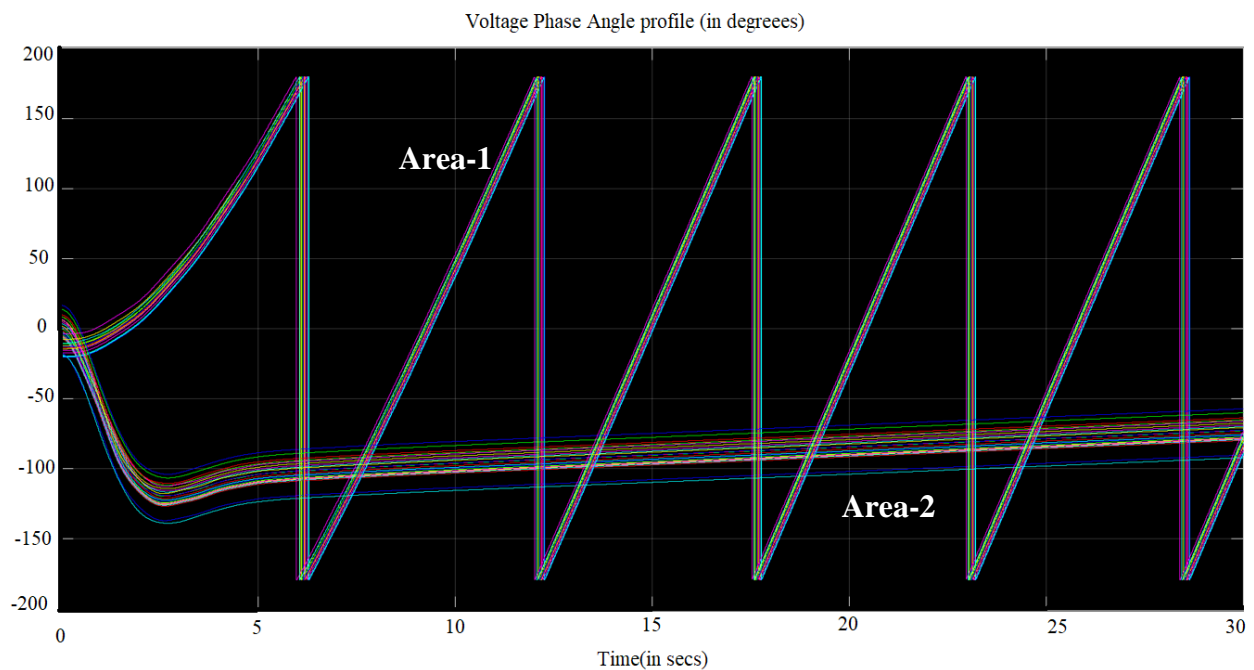


**Fig 4.9:** Voltage phase angle profile prior load control (Scenario-1)

Now the loading conditions have to be modified in order to bring the frequency of the incoming phasor as close to the reference phasor. As in this scenario, the incoming frequency is greater than the reference frequency, the total load to be shed for achieving a frequency close to the reference phasor can be calculated using the equation (14). For calculating this value, the equivalent inertia constant of the multi-machine system (Area-1) has to be calculated first.

The inertia constants of the four generators inside Area 1 are noted in the following table.

Generator Bus number	Inertia constant H (in secs)
30	4.2
37	2.43
38	3.45
39	50

**Table 4.2:** Inertia constants of the various generators in Area-1

The equivalent  $H_{eq}$  of Area-1 amounts to

$$H_{eq} = \sum_{i=1}^n H_i = 4.2 + 2.43 + 3.45 + 50 = 60.08 \quad (20)$$

For testing for this project, the settling time after the overall load change was scheduled to take effect within 5 seconds. Thus plugging in the values in equation 14, the total  $P_{diff}$  or total load change was calculated to be

$$P_{diff_{eq}} = \frac{2H_{eq}}{f_0} \left( \frac{f_{incoming} - f_{reference}}{t_{diff}} \right) = \frac{2 * 60.08}{60} * \left( \frac{60.19 - 60.01}{5} \right)$$

$$\Rightarrow P_{diff_{eq}} = 0.072096 \text{ p.u.} = 72.096 \text{ MW} \quad (21)$$

Note: The Base MVA is taken as 1000 MVA

Hence, the total amount of load to be shed throughout the island is around 72 MW.

Secondly, the order of load shed at the different PQ buses can be decided by the operator either based upon the voltage magnitudes in ascending order or the load availability upon analysis. Next, executing the algorithm for calculating the share at each load bus based upon voltage sensitivity analysis as per equation (18) in the Simulink model, the technique directs the operator to change the loading to following conditions.

Bus Number	Load (in MW)
3	363.2
18	176.7
25	223.4
26	147
27	303.4
28	216.8
29	288.4
39	942.3

**Table 4.3:** Loads at various PQ buses of Area-1 post load control (Scenario-1)

The operator can use these values to change the loading in the order earlier discussed based upon different bus voltage profiles. Once this is achieved, the frequency of the incoming island reduces down to **60.02** Hz (very much closer to the reference frequency). The voltage phase angle profile of the two islands has been modified as follows.

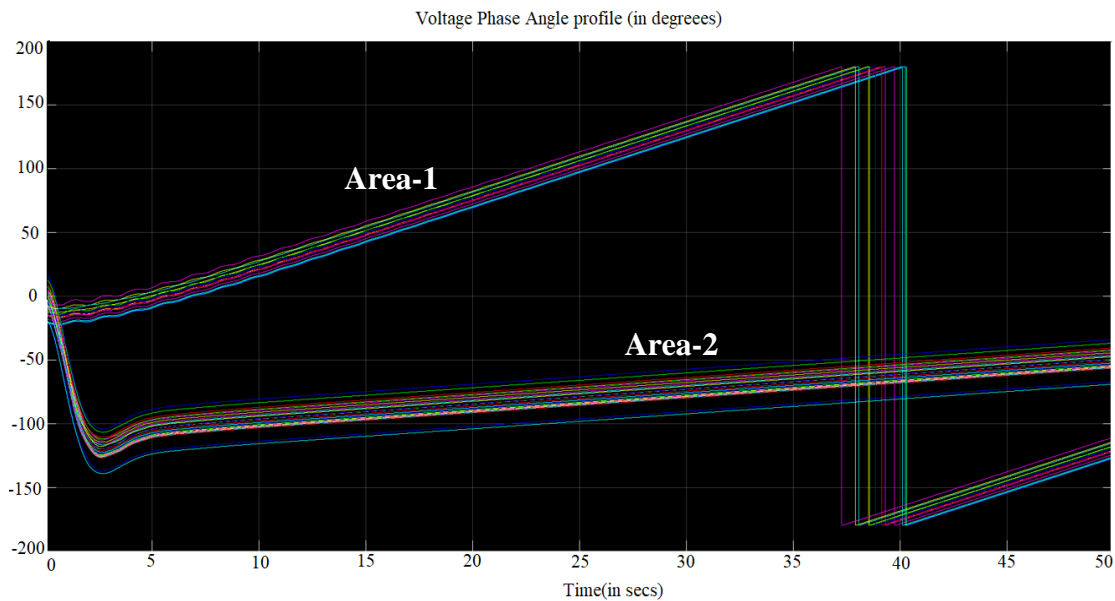


**Fig 4.10:** Voltage phase angle profile post load control (Scenario-1)

The operator can now close the synchronizing breakers if all other conditions for voltage magnitude and angles are within limits and would thus lead to minimal after synchronization transients and much smoother synchronization.

**Scenario-2:**

Now modifying the system conditions and maintaining the loading conditions as depicted below in the table, a frequency of **59.83** Hz for Area-1 (incoming island) is achieved. The following table depicts the loads at the various PQ buses in Area-1 prior load control.

Bus Number	Load (in MW)
3	363.2
18	176.7
25	223.4
26	147
27	303.4
28	216.8
29	288.4
39	1025.346

**Table 4.4:** Loads at various PQ buses of Area-1 prior load control (Scenario-2)

The voltage phase angle profile of the two islands with the incoming phasor frequency lesser than the reference phasor frequency is depicted in the following figure.

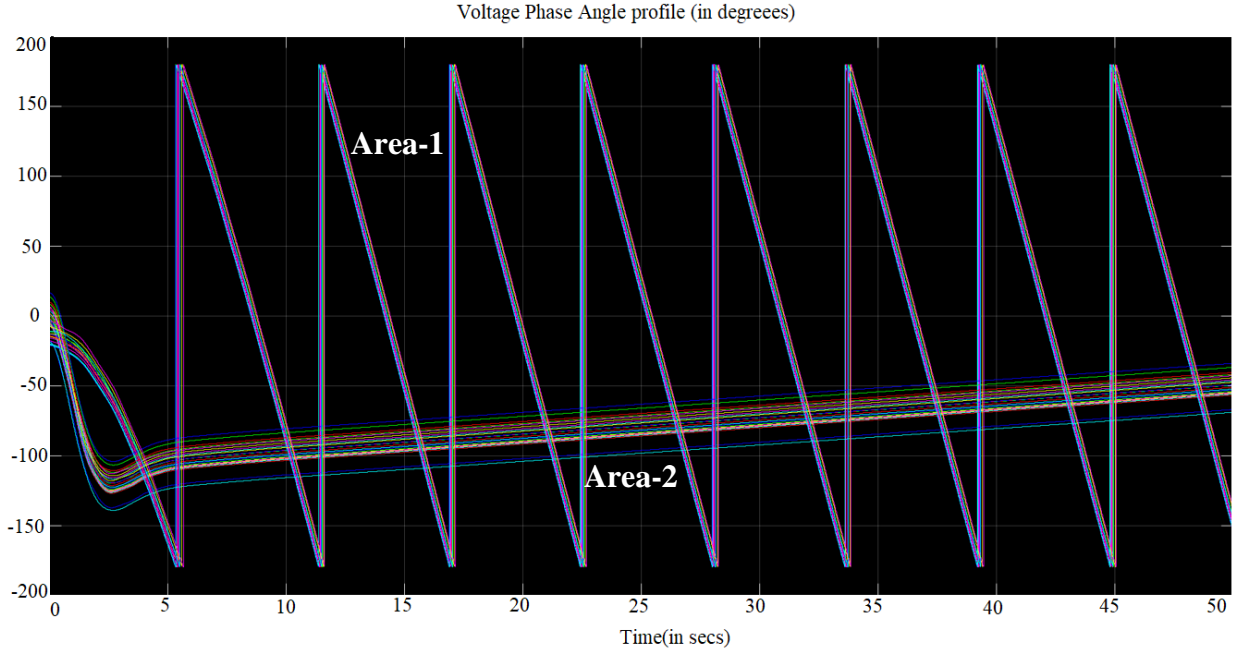


**Fig 4.11:** Voltage phase angle profile prior load control (Scenario-2)

The total load to be incremented throughout the island for achieving a frequency close to the reference phasor can again be calculated using the equation (14).

$$P_{diff_{eq}} = \frac{2H_{eq}}{f_0} \left( \frac{f_{incoming} - f_{reference}}{t_{diff}} \right) = \frac{2 * 60.08}{60} * \left( \frac{59.83 - 60.01}{5} \right)$$

$$\Rightarrow P_{diff_{eq}} = -0.072096 \text{ p.u.} = -72.096 \text{ MW} \quad (22)$$

Thus, the total amount of load to be increased throughout the island is around 72MW.

Now executing the algorithm for calculating the share at each load bus based upon the voltage sensitivities and equation 19 in the Simulink model we see that the technique directs the operator to change the loading to following conditions

Bus Number	Load (in MW)
3	355.7
18	171.7
25	216
26	139
27	295
28	204.4
29	281
39	998.8

**Table 4.5:** Loads at various PQ buses of Area-1 post load control (Scenario-2)

Once the loading is changed as per these requirements, the frequency of the incoming island rises to **60.00 Hz** (very much closer to the reference frequency). The voltage phase angle profile of the two islands has been modified as follows.

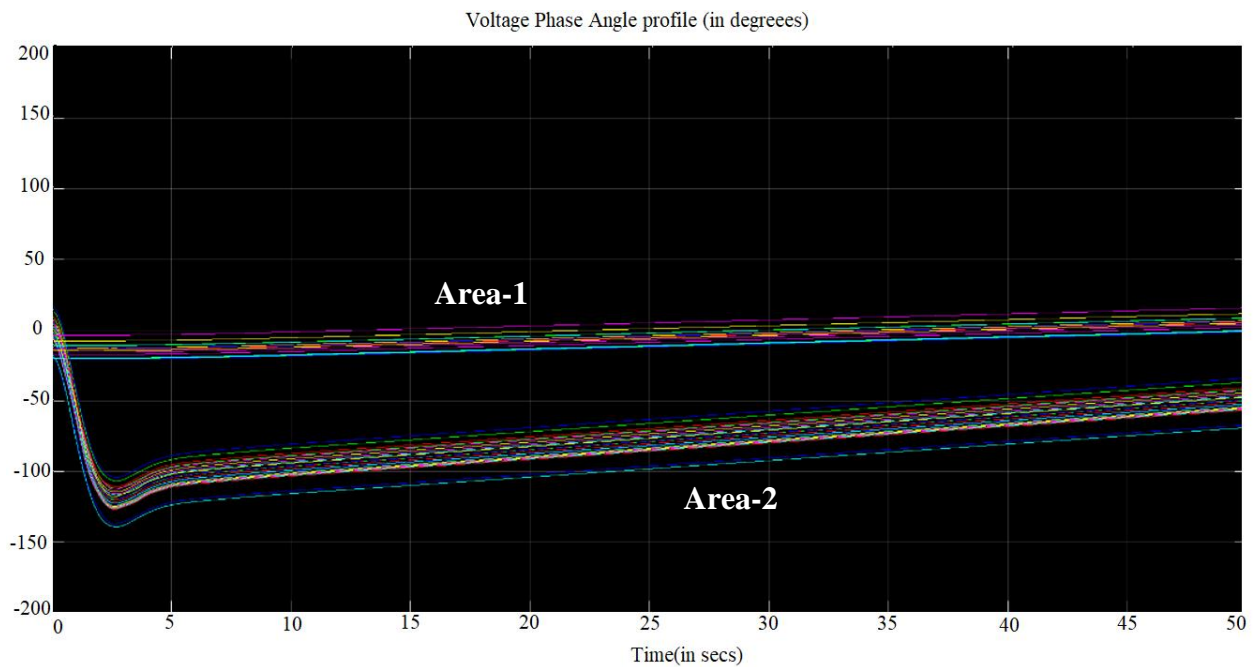


**Fig 4.12:** Voltage phase angle profile post load control (Scenario-2)

The technique was found to be quite effective in regulating the frequency of the incoming island as desired. The most important thing to consider such a technique is because of a blackstart scenario during which the utilities have ample control of changing or modifying the loads across different areas which might not be feasible during normal scenarios. However, the purpose of inclusion of such a technique is to show how any control technique can be incorporated into the synchroscope and can be tailor-made for specific utilities as required.

The after synchronization transients were minimal and led to smoother and successful synchronization in both the cases.



**Fig 4.13:** Smoother synchronization with inclusion of load control

# Chapter-5: Conclusion and Future Work

## 5.1 Conclusion

This thesis document discusses the implementation of a synchrophasor based centralized remote synchroscope (otherwise referred to as PMU synchroscope in the document) as a part of the development of analytics for the DOE-sponsored openECA project. The basic idea to achieve such functionality at a remote central location (such as the utility's control room) was to overcome the various delays associated in a wide area measurement system, which would have eventually hindered the accurate time synchronized breaker closing action at the substation. The concept of advanced angle was used and a modified synchroscope application supporting all features of the traditional physical synchroscope with the inclusion of some additional features was created which can be used for immediate implementation if required in the utility sector compatible to the openECA platform. The synchroscope restricts the chances of errors made on behalf of the user/operator and raises appropriate annunciations/alarms to notify how much of a change is required for the measurements of the two buses to be synchronized. In order to demonstrate how to achieve these modifications (which ultimately would be user/utility specific procedures), a load control technique based on the algorithm stated in [21] is used with minor modifications. Satisfactory results were obtained with the inclusion of such an algorithm. The after synchronization transients were minimized and hence, leading to much smoother and successful synchronization. However, the important point to note is that this type of technique would be more feasible for the utility during blackstart or bulk power system restoration as they would have much more flexibility on loads during this time as compared to normal situations.

## 5.2 Future work

The openECA application along with most of the analytics associated with it are a part of the open source project. The PMU synchroscope developed was built in C# language and has been uploaded to the GITHUB site, and the web links are provided in the appendix. This provides a great opportunity for power system researchers or utility personnel to look on the web and can start modifying the application to tailor fit as per their requirements. The most crucial modification that can be added to this project is the inclusion of real-time downstream delays for the channel to be used to send back the breaker commands in the GUI of the synchroscope. This would further reduce error on behalf of the user and would lead to much smoother and more successful time synchronization between the two buses. Apart from that, as voltage control and frequency control were beyond the scope of this project, possible future work might be the inclusion of these aspects within the PMU synchroscope application, which might be custom made individual utility differently, depending upon their system parameters and system topology. In this way, a more comprehensive delay incorporated PMU synchroscope for the ease of the user/operator can be built.

## References

- [1] R. J. Campbell, “Weather-Related Power Outages and Electric System Resiliency,” Washington DC, USA: Library of Congress, 2012.
- [2] S. H. Conrad, R. J. LeClaire, G. P. O’Reilly and H. Uzunalioglu, “Critical national infrastructure reliability modeling and analysis,” Bell Labs Tech. J., vol. 11, no. 3, pp. 57–71, 2006.
- [3] E. Mills. “Electric grid disruptions and extreme weather.” [Online]. Available: <http://evanmills.lbl.gov/presentations/Mills-Grid-Disruptions-NCDC-3May2012.pdf>
- [4] M. M. Adibi and L. H. Fink, “Overcoming restoration challenges associated with major power system disturbances—Restoration from cascading failures,” IEEE Power Energy Mag., vol. 4, no. 5, pp. 68–77, Sep. 2006.
- [5] M. M. Adibi and L. H. Fink, “Power system restoration planning,” IEEE Trans. Power Syst., vol. 9, no. 1, pp. 22–28, Feb. 1994.
- [6] Feng Qiu, Peijie Li, “An Integrated Approach for Power System Restoration Planning,” Proceedings of the IEEE, 2017.
- [7] Qin Zhijun, Liu Shanshan, Hou Yunhe, “Virtual Synchroscope: a novel application of PMU for system restoration,” 2011The International Conference on Advanced Power System Automation and Protection.
- [8] S. Kolluri, S. Mandal, F. Galvan, and M. Thomas, “Island formation in Entergy power grid during Hurricane Gustav” in Power & Energy Society General Meeting, 2009. PES '09. IEEE, 2009, pp. 1-5.
- [9] S. Corsi and C. Sabelli, “General blackout in Italy Sunday September 28, 2003, h. 03:28:00” in Power Engineering Society General Meeting, 2004,IEEE, 2004, pp. 1691-1702 Vol.2.

- [10] “Final Report of the Investigation Committee on the 28 September 2003 Blackout in Italy,” UCTE Report – April 2004.
- [11] Konstantinos Diakos, Qiuwei Wu, Arne Hejde Nielsen, “Phasor Measurement Unit and Phasor Data Concentrator test with Real-Time Digital Simulator,” 2014 IEEE PES Asia-Pacific Power and Energy Engineering Conference (APPEEC)
- [12] IEEE Guide for Phasor Data Concentrator Requirements for Power System Protection, Control, and Monitoring.
- [13] Richard C Schaefer, “Art of Generator Synchronizing,” IEEE Transactions on Industry Applications, 2017.
- [14] Michael J. Thompson, “Fundamentals and Advancements in Generator Synchronizing Systems,” 2012 65th Annual Conference for Protective Relay Engineers.
- [15] Daniel L. Ransom, “Get in Step with Synchronization,” 2014 IEEE/IAS 50th Industrial & Commercial Power Systems Technical Conference.
- [16] C. W. Taylor, V. Venkatasubramanian, and Y. Chen, “Wide-area stability and voltage control,” in Proc. 2002, 7<sup>th</sup> Symp. Specialists in Electric Operational and Expansion Planning, pp. 1–9.
- [17] F. Zhang, Y. Sun, L. Cheng, X. Li, J.H. Chow, and W. Zhao, “Measurement and Modeling of Delays in Wide-Area Closed-Loop Control Systems,” 2015 IEEE Transactions on Power Systems
- [18] W. Liu, H. Luo, S. Li, and D. Gao, “Investigation and modeling of communication delays in wide area measurement system,” in Proc. 2012 Asia-Pacific, Power and Energy Eng. Co
- [19] Z. Hu, X. Xie, J. Xiao, and L. Tong, “Analysis and test on delays in the wide area measuring system,” Autom. Elect. Power Syst., vol. 28, no. 15, pp. 39–43, 2004.nf. (APPEEC), pp. 1–4.

- [20] Prithwish Mukhopadhyay, Pushpa Seshadri, Chitranshi Gangrekar, Chandan Kumar, Awani Bhusan Rai, Naveen M. Reddy, “WAMS and Synchrophasor experience during synchronization of Large grids in India,” 2015 IEEE International Conference on Signal Processing, Informatics, Communication, and Energy Systems (SPICES).
- [21] Poonam Joshi, “Load Shedding Algorithm Using Voltage and Frequency Data,” Master’s Thesis, Clemson University, 2007.
- [22] <https://www.opal-rt.com/systems-ephasorsim>
- [23] M. Parniani, A. Nasri, “SCADA based under frequency load shedding integrated with rate of frequency decline,” 2006 IEEE Power Engineering Society General Meeting.
- [24] D Yang, Z Nie, K Jones, V Centeno, “Adaptive decision-trees-based regional voltage control,” 2017 North American Power Symposium (NAPS).
- [25] Duotong Yang, Dissertation on “A Data Analytics Framework for Regional Voltage Control,” 2017 Virginia Tech.
- [26] Hung-Ming Chou, Chetan Mishra, Yajun Wang & Michael K. Thomas, “Application of RTDS as Real-Time Decision Support Tool,” Grid of the Future Symposium, 2017 CIGRE.
- [27] Anamitra Pal, Chetan Mishra, Anil Kumar S Vullikanti & SS Ravi, “General optimal substation coverage algorithm for phasor measurement unit placement in practical systems,” 2017 IET Generation, Transmission & Distribution, 11, 347-353.
- [28] Dao Zhou, Jiahui Guo, Ye Zhang, Jidong Chai, Hesun Liu, Yong Liu, Can Huang, Xun Gui, Yilu Liu. “Distributed Data Analytics Platform for Wide-Area Synchrophasor Measurement Systems”, IEEE Trans. Smart Grid, 2016, 2397- 2405.

# Appendix

## Related Links

[1] <https://github.com/GridProtectionAlliance/openECA>



[2] <http://www.opal-rt.com/systems-phasorsim>



[3] [https://github.com/tapasbarik/Analytics/blob/master/PMU\\_Synchroscope\\_Final.zip](https://github.com/tapasbarik/Analytics/blob/master/PMU_Synchroscope_Final.zip)

